Fatigue characterization of multiple delaminations

Master Thesis

Alejandro Hernandez del Valle
Design of Mechanical Systems
Aalborg University

1/06/2023

AALBORG UNIVERSITET
STUDENTERRAPPORT

Master thesis
Design of Mechanical Systems
Fibigerstræde 16
9220 Aalborg
www.mp.aau.dk/

Title:

Fatigue characterization of multiple delaminations

Project:

Master Thesis

Project Period:

1. February - 1. June

Students:

Alejandro Hernandez del Valle

Supervisors:

Esben Lindgaard

Simon Mosbjerg Jensen

External examiner:

Lars Erik Bräuner

Report page number: 43
Appendix page number: -
Total page number: 43
Completed: June 1, 2023

Abstract:

This thesis investigates whether the overall toughness of the material can be improved by promoting multiple delaminations. This is done by first investigating state-of-the-art methods regarding materials that exhibit toughening behaviour during fracture initiation. This behaviour can be achieved by introducing weakening patches between the material interfaces. In order to validate the results found in the literature, experimental testing of a glass fiber reinforced polymer (GFRP) double cantilever beam (DCB) containing a weakening patch configuration was conducted. These DCB specimens were tested under quasi-static and fatigue loading conditions. The results showed that under quasi-static loading, no toughening was observed in the DCB beams tested. In the context of fatigue testing, the characterization of this test revealed toughening behaviour in the test specimens. These studies proposed a novel contribution to state-of-the-art methods by providing a new benchmark case for the study and prediction of multiple fatigue-driven delaminations in GFRP specimens.

Preface

This project is written as a Mechanical Engineering project report for 4^{rd} semester of Masters in Design of Mechanical Systems at Aalborg University.

The author wishes to thank her thesis supervisor, Associate Professor Ph.D. Esben Lindgaard, and Post.Doc Simon Mosbjerg for their significant inspiration, advice, and support throughout this project.

Furthermore, the author wishes to thank the workers at Aalborg University's Materials and Production workshop for their assistance in the manufacturing and testing of the DCB specimens.

Alejandro Hernandez del Valle

List of Figures

Contents

Introduction 1

1.1 Background and motivation

Composite materials are compounded by two or more different materials to create a new one, which often has better properties. These types of materials are most widely used in multiple industries such as aerospace, automotive, and construction industry due to their strength-to-weight ratio, corrosion, wear resistance and strength [1].

Composite materials offer a significant advantage in terms of mechanical properties in comparison to conventional engineering materials, such as steel. Unlike engineering materials, composites are mostly heterogeneous and anisotropic, meaning that their properties are non-uniform and they have distinct material properties depending on the fiber directions [1].

Among the various types of composite materials that exist, this thesis will be focused on Fiber Reinforced Polymers (FRP), which are materials composed of fibers bonded to a matrix. Through this bonding process, the fiber and the matrix properties are combined to create a new material which enhanced them. Typically, the fibers are responsible for carrying the primary load, while the matrix serves to bond the fibers together and facilitate the transfer of load between them [2].

As the need for lightweight and more efficient structures has increased, composites have been introduced into various industries, resulting in new composite design philosophies. Bragal et al. [3] state three different design concepts that have been evolving through the years: safe-life, fail-safe and damage tolerance philosophy.

Safe-life and fail-safe design philosophies are commonly used design philosophies. These philosophies usually account for not considering damage within the material useful life, which in some cases has led to disastrous failures. The use of these philosophies results in significant expenses when utilizing equipment designed under these philosophies [3], [4].

Damage tolerant design philosophy accounts for initial damage that has occurred in the structure. This damage makes it necessary to take this early damage stage into account when determining inspection criteria and intervals. Damage tolerant designs are frequently used because they provide more adaptation and flexibility to overcome uncertainty. By reducing the need for maintenance or replacement, this design strategy can increase safety and reliability while at the same time lowering costs [3],[5].

Damage tolerant philosophy is related to high cyclic loading. Yet, compared to isotropic materials, like metals, the fatigue behaviours of composite materials are very different. The initiation of microcracks in composite materials occurs at the early stages of loading, yet composites are still able to bear the load until final failure [6]. This philosophy also deals with crack growth, which is thought of as the separation of surfaces between any two laminates of a composite laminate. This phenomenon is known as delamination [7].

Understanding the qualities of the materials and the structural requirements can help to create a better damage tolerant structure utilizing damage tolerant materials. These damage tolerant materials take into account the strength beyond the linear elastic limit, allowing damage to be detected and the structure to be repaired or replaced before it reaches its design stress. To create damage tolerant structures, materials that exhibit toughening behaviour during fracture initiation and progression are particularly well suited to the damage tolerance design philosophies presented [5].

1.2 Failure in composite materials

Considering the damage tolerance design philosophy mentioned in the previous section, an understanding of the different failure mechanisms is required to be able to use and design a damage tolerance material.

With respect to failure mechanisms in composite materials, a distinction between inter-lamina and intra-lamina failure mechanisms needs to be done. Intra-lamina occurs within a single layer of the composite material. On the other hand, inter-lamina occurs between two or more adjacent layers of the composite material.

Intra-lamina failure usually includes fiber and matrix failure. Fiber failure can occur due to excessive tensile or compression loading creating failures such as fiber matrix debond and kink band. The failure that occurs in a lamina does not extend to the adjacent layers.

Intra-lamina failure usually happens under different loading conditions and may include failures such as shear failure, transverse cracking and buckling [1]. The most common failure regarding inter-lamina mode is delamination, which happens when a lamina debonds from the adjacent layers [8].

Due to the high level of fibre composition in composite materials, delamination is one of the most serious failure mechanisms that can shorten the life of the material [9]. Delamination is a difficult failure mechanism to detect by non-destructive inspection because it is usually embedded in the whole structure. This defect usually occurs during the manufacturing process but can also occur when the composite is in service or even as an external factor [10], [11].

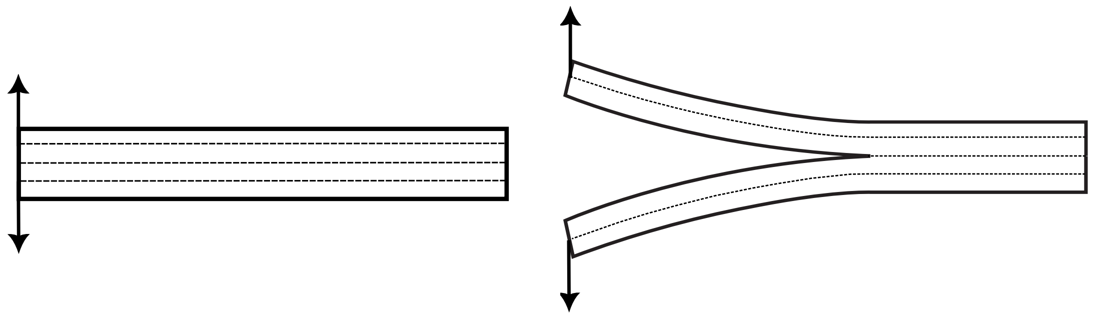

(a) Intact material *(b)* Delaminated material

Figure 1.1. Delamination of a fiber-reinforce composite material under arbitrary loading conditions.

Delamination can be interpreted as a growing crack between the laminate surfaces as shown in Figure 1.1. Fracture mechanics can be used to study the phenomenon of delamination as it can be considered as a growing crack problem [12], which implies that it only propagates through one interface. Delamination in composites is a complex process caused mainly by the composite orthotropic properties, mixed mode cracking, and crack bridging [13], [14].

The analysis of crack growth problems in composites usually involves fibre bridging. Large scale bridging depends mainly on the specimen geometry and material properties of the laminate [15]. This phenomenon is usually located in the crack wake and causes an increase in fracture resistance as the crack grows [16]. Fiber bridging can be seen in Figure 1.2.

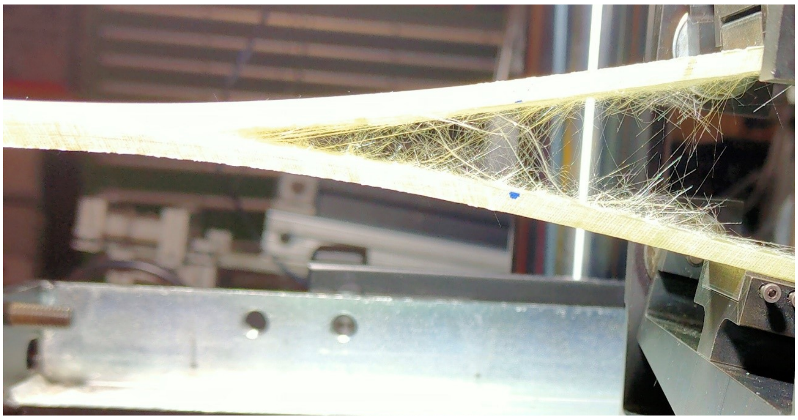

Figure 1.2. Fiber bridging phenomenon of a fiber reinforced composite.

Mechanically, crack bridging can be described in terms of tensile separation laws. It is still a challenge to measure traction-separation laws and use them in structural design. This damage is localised and is known as the fracture process zone because delamination is considered to be a separation of bound layers.

Traction separation laws dictate that less traction can be transmitted through the fibres as the separation of the layers increases, as shown in Figure 1.3. Traction separation laws are commonly considered to be a material property that has the same behaviour throughout the fracture process zone that occurs in the material [5].

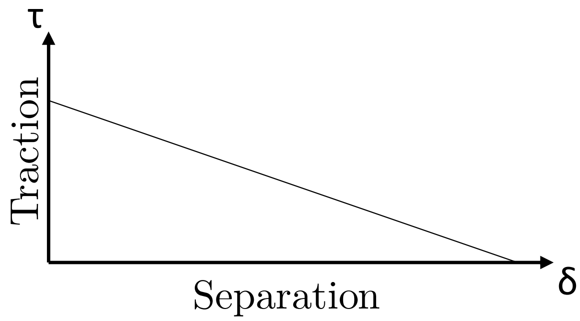

Figure 1.3. Linear traction-separation law [12].

The delamination phenomena can be analysed using fracture mechanics [12]. Since delamination is related to crack growth, it should be considered as a stable process and the load required to generate unstable crack growth should be higher than the load required to initiate it. Crack growth occurs when the energy consumed by the fracture process is greater than the energy dissipated by the structure.

1.3 Analytical solution for one delamination

Now that the material failure mechanism have been explained, an analytical solution for a DCB (Double cantilever beam) with one delamination case is studied. This study provides an theoretical understanding on how a DCB responds to crack propagation. The DCB geometry used for this analysis is shown in Figure 1.4

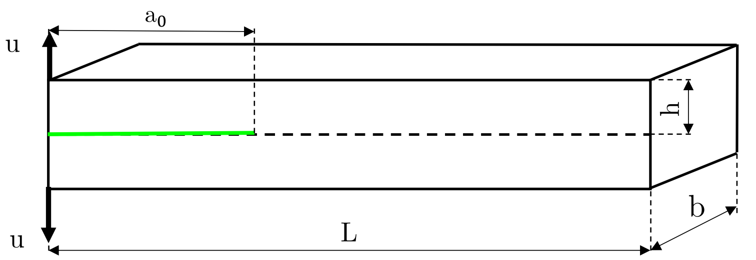

Parameters	[mm]
a_0	100
h	4
b	30

Figure 1.4. Geometry and parameters of the DCB.

Figure 1.4 includes the main parameters intervening in the analytical solution, being a_0 the initial crack length, h half of the thickness and b the width. The total length of the beam is L but for this study is not a needed parameter.

This analytical solution is based on a mode I loading with displacement control conditions. This means that the crack faces are separated due to an imposed displacement. The material properties are the same as the used in [16], which the used properties are shown in Table 1.1.

Table 1.1. Glass fiber-reinforce polymer material parameters.

Parameters	Definition	Value
E_{11}	Young Modulous in the Fiber direction	$21.5 \cdot 10^9$ Pa
E_{22}	Young Modulous transverse to fiber direction	$10 \cdot 10^9$ Pa
G_{13}	In-plane shear modulus	$4 \cdot 10^9$ Pa
G_c	Critial energy release rate	2000 J$/m^2$

In order to solve this problem, the solution is based on the calculation of the energy release rate which can be defined as the energy loss per unit of the specimen length for an increase in the delamination growth. This can be mathematically represented as shown in Eq. 1.1

$$G = -\frac{1}{b}\frac{dU}{da} \tag{1.1}$$

Based on the ASTM D5528-01 standards [17], G$_{Ic}$ value can be calculated in various ways, but the proposed method is the Modified Beam Theory (MBT) since it provides more conservative values. The formula for mode I G$_I$ for a perfect clamped DCB is shown in Eq. 1.2

$$G_I = \frac{3P\delta}{2ba} \tag{1.2}$$

Where P is the reaction forces due to the displacement δ, and a is the crack propagation. However, this solution does not account for the displacements due to shear deformation and for local deformations that can appear around the crack tip. In order to solve this problem, Harper et al. [18] proposed a corrected beam theory that accounts for these features. From this theory, the displacement of the crack tip can be represented as shown in Eq.1.3.

$$\Delta_I = \frac{2Pa^3}{3E_{11}I} \tag{1.3}$$

Where Δ_I is the displacement of the crack tips and I is the second moment of inertia *($bh^3/12$)*. To correct the displacement shear deformation and local deformation, Eq.1.4 is presented.

$$\Delta_I = \frac{2P(a+\chi(2h)^3}{3E_11I} \tag{1.4}$$

Where χ is the correction parameter, which was determined analytically by Reeder et al. [19].

$$\chi = \sqrt{\frac{E_{11}}{11G_{13}}\left[3-2\left(\frac{\Gamma}{1+\Gamma}\right)\right]}, \qquad where \qquad \Gamma = 1.18\frac{\sqrt{E_{11}E_{22}}}{G_{13}} \tag{1.5}$$

From these equations, the energy release rate can be calculated as shown in Eq. 1.6.

$$G_I = \frac{P^2(a + \chi(2h)^2}{bE_{11}} \tag{1.6}$$

From the previous equations, the load-displacement curve can be now determined, by linearly increasing the displacement and the load until reaching G = G_{Ic}. From this point, the delamination phenomenon starts. The load-displacement response is shown in Figure 1.5.

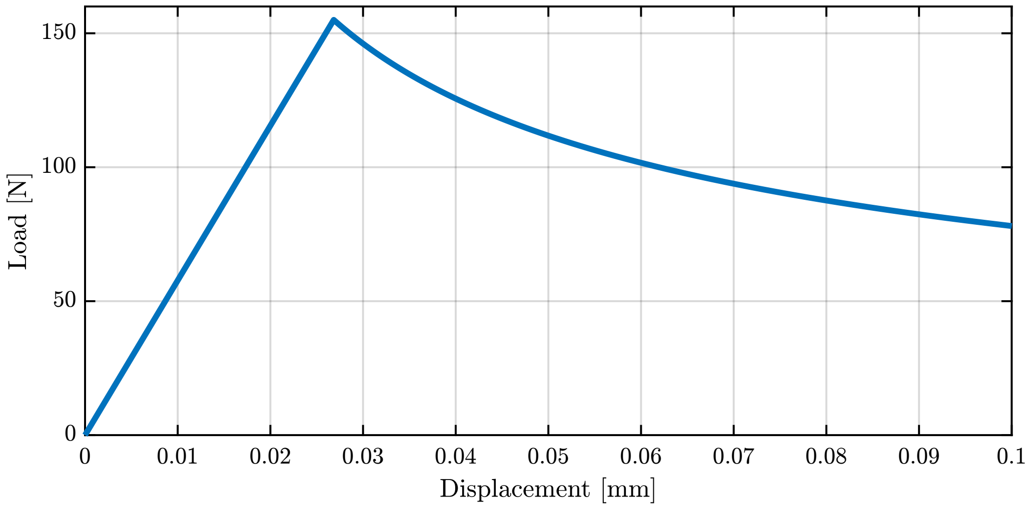

Figure 1.5. Load-displacement curve for a GFRP DCB with one delamination.

Figure 1.5 shows a linear behaviour during the loading phase, this linear behaviour changes when G reaches G_{Ic}. After this moment, the crack starts to propagate and the load starts to decrease as the crack tips continue to separate from each other.

However, it is possible to increase the fracture toughness of the material by creating interface patches that initiate multiple delaminations, being this a suitable option to achieve a damage tolerance material [20].

1.4 Material toughening due to multiple delaminations

As mentioned in previous sections, the damage tolerance design for a composite material can be modified to have a toughening behaviour once multiple cracks are developed in the interface. These cracks are developed due to delamination, which happens due to weak interfaces and is usually one of the main reasons for failure in composites [8]. In order to minimize this phenomenon, various methods can be found in the literature. These methods are related to interface toughening.

Sørensen et al.[21] investigate crack propagation in GFRP specimens. In this work, the fracture energy of a pre-made crack was analyzed under mode mixity conditions. In the early stages, fiber bridging appeared as the crack propagate through the interface.

Later on, a second crack emerged at the laminate next interface, with its associated fiber bridging. The main result obtained from this test is that this second fiber bridging increased the crack growth resistance of the whole specimen.

Goutianos et al.[22] explore the introduction of weak planes that result in repeated delaminations to enhance the laminate overall fracture resistance. This was done by making a validation between an analytical and a numerical model. The analytical model based on the J-integral showed a linear relationship between the number of delaminations and the increase in fracture toughness. The model was further validated with the numerical model. However, in the numerical models, it was discovered that the fracture toughness also depended on the geometry and interface features making the fracture toughness not linearly increased with the number of delaminations.

Trabal et al. [20] investigate the toughness increase by inserting toughening and weakening patches into the composite to induce multiple delaminations. This was carried out by numerical parameter study over a DCB in which toughening and weakening patches were included. This study was made in function of different interface properties such as onset traction and the critical energy released rate. This results in a toughening effect for the whole laminate promoting multiple delaminations.

These interface patches, increase the life of the specimen under higher load compared to not having patches. As for the weakening patch, the completed analyses yielded promising outcomes, making the suggested method an intriguing choice to obtain damage tolerance by strengthening laminated against delamination growth [20].

The previously stated method has only been studied numerically, and so experimental verification needs to be done to confirm that the growth of multiple delaminations can promote a higher toughness of the total structure.

1.5 Fatigue in Composite Materials

The use of composite materials in various industrial sectors has increased the importance of fatigue research in this field, as mechanical systems frequently face cyclic stresses [6]. There is a great difference in fatigue behaviour between metals and composites.

In service, homogeneous and isotropic materials, such as metals, appear to retain their stiffness, but when the first crack appears, these materials enter the final stage, as a cracked system can cause the entire system to fail.

In composite materials, damage can manifest at an early stage and spread throughout the material, resulting in a reduction of stiffness within the damaged zone. Instead of leading to total system collapse, cracks in laminates can be used to reduce stress concentration in the fibres [23], [24].

Understanding the fatigue behaviour of composite materials is necessary to ensure their safety. As a consequence, the development of fatigue models has accompanied the growth of composite applications. Diegrieck et al.[24] classified the fatigue models developed into three categories: fatigue life models, phenomenological models, and progressive damage models.

- Fatigue life models: The total fatigue of the system is calculated using S-N curves.
- Phenomenological models: Describe how properties such as strength and stiffness decrease through observation of the macroscopical properties.
- Progressive damage models: Can predict the growth of the actual damage characterization, such as intra-lamina and inter-lamina failures.

This analysis is based on the progressive damage models. Using this approach, the range of acceptance of composite structures increases; and failures, such as delaminations, are accepted [24]. As stated in previous sections, delamination is one of the most common failure mechanisms in composite materials.

Since this failure mechanism is highly common since various numerical implementations reviews can be found in the literature [24], [25]. For the experimental fatigue testing, the delamination test is based on the data obtained from the experiments; where the crack propagation a is obtained as a function of the number of cycles. This data is used to express the crack growth rate (da/dN), where it is represented in terms of the stress intensity factor as shown in Figure 1.6 [25].

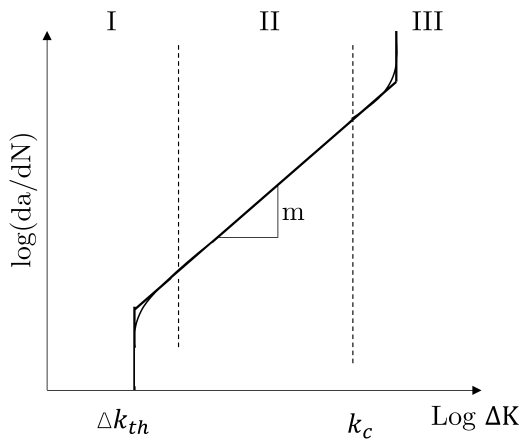

Figure 1.6. Crack growth rate in terms of the stress intensity factor.

The crack growth curve represented in Figure 1.6 shows three main areas. The first represents the crack initiation, followed by the crack propagation and finishing on the critical load region. In composite materials, more specifically in fiber-reinforce polymer, the region corresponding to the propagation part (stage II) is highly sensitive. For this reason, a minor uncertainty in the test experiment can produce a difference in the results for the crack growth rate [14].

The fatigue characterization of the delamination phenomenon which corresponds to Section II in Figure 1.6, uses the *Paris Law* to describe the crack growth rate [31]. Paris law shows the relationship between the crack growth rate (da/dN) and the stress intensity factor range ($\Delta K = K_{max} - K_{min}$) as shown in Eq.1.7.

$$\frac{da}{dN} = C(\Delta K)^m \tag{1.7}$$

Where a corresponds to the crack length, N is the number of cycles, C and m are material parameters. Since the Paris Law has been used for metals, its success has led to the Paris Law also being used in composite materials. The complexity of calculating the SIF for fiber reinforced polymers makes SERR the primary factor in delamination growth modelling [14]. Since SERR is used in simulations to validate the data, it can also be measured in experiments, being the most used term to characterize crack propagation due to fatigue loading. Considering this, the Paris law equation can be rewritten in terms of SERR as:

$$\frac{da}{dN} = C(G_{max})^m \tag{1.8}$$

Problem statement 2

As previously mentioned in Chapter 1, delamination is one of the main failure mechanisms found in composite materials. However, the appearance of delamination does not account for the total failure of the structure. Considering the damage tolerant design, the life of the structure can be extended using this philosophy. This can be done through the toughening of the structure by interface toughening methods.

In Section 1.4 a literature review explaining the different toughening methods is done, where it was shown that a way of toughening the whole structure is achieved by adding weakening and toughening patches in the structure interface. With the inclusion of these patches, it was observed that multiple delaminations were onset, improving the overall toughening of the damaged structure.

According to the work presented by Trabal et al. [26], [20], the incorporation of the weakening and toughening patch increases the total toughness of the structure. This work is done under quasi-static loading conditions were further experimental work needs to be done. Also, Trabal et al. [27] propose a novel numerical fatigue study in which the structure weakening patch is studied under fatigue loading conditions.

Thus, this thesis considers the possibility of improving the toughness of a structure by promoting multiple delaminations under fatigue loading conditions. The global scope is to make a new benchmark case for the study and prediction of multiple fatigue-driven delaminations in GFRP specimens. The aim is to make a novel contribution to the state-of-the-art, beyond the existing research on the subject. To the author knowledge, no experimental testing of multiple fatigue-driven delamination tests are available in the literature.

2.1 Objectives

The objective of this thesis is to provide a new benchmark case for the study and prediction of multiple fatigue-driven delaminations in GFRP specimens. Following this research path, multiple objectives were initially set.

- Design and manufacture several GFRP specimens containing weakening patches.
- Conduct a quasi-static loading on a Double Cantilever Beam (DCB) with multiple delaminations using glass-fibre reinforced polymer (GFRP) to determine the fatigue study parameters.
- Conduct fatigue load testing on a Double Cantilever Beam (DCB) with multiple delaminations using glass-fibre reinforced polymer (GFRP) specimens.
- To perform a fatigue characterization from the test obtained data.

Numerical solutions for multiple delaminations 3

In section 1.4, an overview of the different toughening methods for a composite material is introduced. This is done through the introduction of weakening and toughening patches through the interface of the composite materials. For this thesis, only the study of weakening patches is considered.

The different studies that have analysed this phenomenon are mainly based on numerical implementation since no experimental work has been developed yet. These numerical implementations are based on mode I and mixed-moded loading cases. In the literature, various numerical analyses of different beam configurations can be found. This chapter introduces an explanation of the numerical solutions for a multiple delamination case for a DCB.

The multiple delamination cases for a DCB are based on the benchmark model proposed by Alfano et al. [28]. The geometry and loading conditions as well as the positioning of the cracks and crack tips are shown in Figure 3.1.

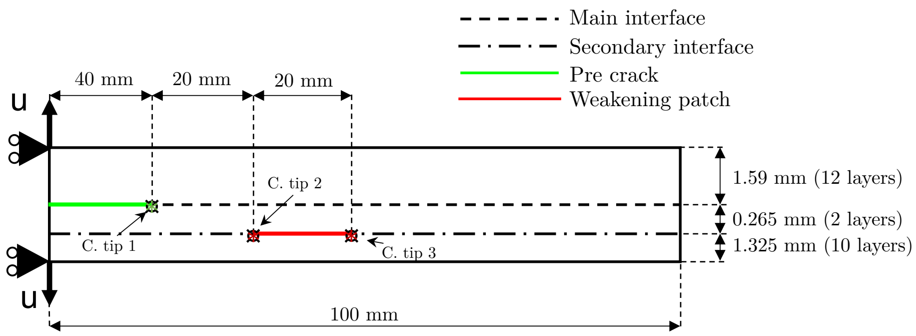

Figure 3.1. Geometry, loading conditions and crack placement of the multiple delaminations DCB. (Adapted from [28]).

Figure 3.1 shows the layer layup as well as the positioning of the different cracks and crack tips. The first crack (green), is placed on the middle plane of the specimen between the 12^{th} and 13^{th} layers, which is referred to as the *main interface*. The second one (blue) is placed on the right side of the first one -two layers beneath-, which interface is referred to as *secondary interface*. In total, this geometry contains 3 different crack tips, the first one is located in the first crack. The second crack contains two crack tips, located at the left and right sides of the *secondary interface* crack.

3.1 Quasi-static loading case

To be able to study the toughening of the materials with the introduction of weakening patches, and the different cracks tips propagation, a quasi-static loading test is performed. This test provides an understanding of the overall response of the system.

In their study proposal, Trabal et al. [26] made a comparison between two finite element implementations. To compare these different approaches, some benchmark problems are analyzed. In those benchmark models, a numerical quasi-static loading case for the described configuration shown in Figure 3.1 is examined. The equilibrium curve as well as the shape of the material during the quasi-static analysis are shown in Figure 3.2.

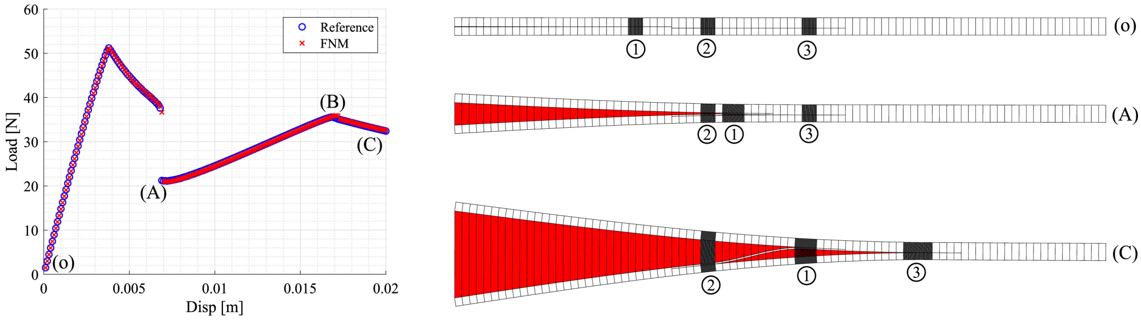

Figure 3.2. Quasi-static loading response of the DCB. Left: load displacement curve, right: deformed stage of DCB [26].

Figure 3.2 is characterized by three main stages which are stage A, stage B and stage C. Also, in Figure 3.2, three different crack tips are considered. The *main interface* crack tip is represented as ①, while ② and ③ are crack tips of the weakening patch located in the *secondary interface*.

In the first analysis stage, a quasi-static loading phase of the DCB is done, which is characterized by the propagation of the ① crack tip.

Once the crack tip ① reaches the crack tip ②, an unstable crack growth of ① is observed. This results in a decrease in the load axis in the equilibrium curve. Then, crack tip ① surpasses crack tip ② during the unstable crack growth reaching stage (A) and starting the delamination of crack tip ③.

Once stage (A) is reached, another quasi-static loading stage takes place until reaching stage (B). This stage is characterized by the further propagation of crack tip ①. The increasing propagation of the crack tip ① together with the onset of crack ③ characterizes this stage. After this stage, a softening behaviour of the material was observed due to the delamination of both cracks.

At the end of the quasi-static loading test, stage (C) is reached; where the crack tip ② remains static and no propagation is seen. For crack tip ① is fully propagated and is located in between the other two crack tips. For crack tip ③ it propagates taking over crack tip ① and propagating further in the specimen.

3.2 Fatigue loading case

Now that the quasi-static loading test has been analyzed, the DCB featuring the triple delamination propagation based on the model proposed by Alfano et al.[28], is studied under fatigue loading conditions. In this implementation, Trabal et al. [27] proposed an innovative study, studying this benchmark problem under fatigue conditions.

The fatigue loading test consists of four blocks, two quasi-static loading blocks and two fatigue loading blocks. The test is performed in a variable amplitude range. Thus, the amplitude in both stages changes. This loading spectrum is shown in Figure 3.3.

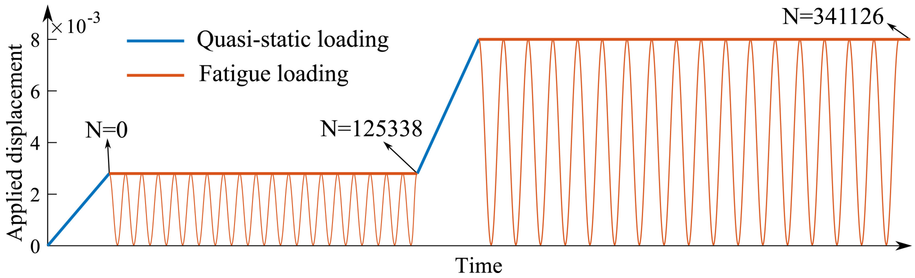

Figure 3.3. Applied displacement imposed to the DCB specimen with respect to time [27].

Figure 3.3 shows the different loading stages and the number of cycles corresponding to each of the stages. In addition, it shows the two quasi-static loading cases which take place before the fatigue stages. The relation between the load and displacement with respect to the load spectrum is shown in Figure 3.4.

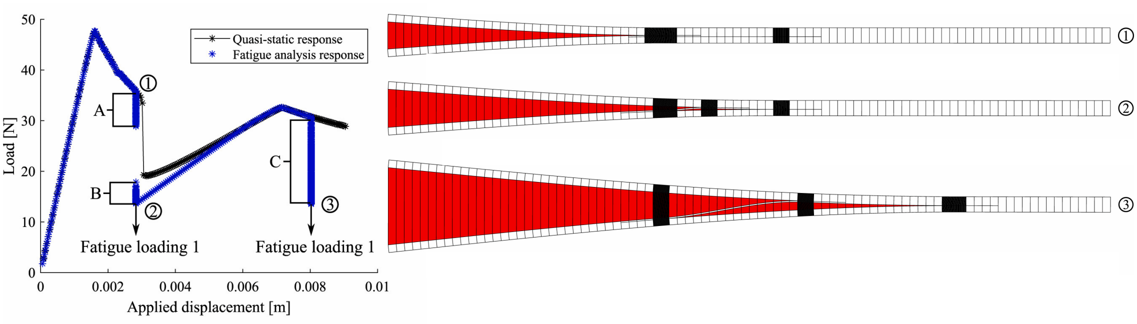

Figure 3.4. Fatigue loading response of the DCB with multiple delaminations. (Adapted from [27])

The fatigue response curve in Figure 3.4 shows that even though a fatigue loading test is performed, multiple delaminations can be obtained. The loading procedure is based on the same principle as the quasi-static loading case.

First, a loading stage is imposed on both exterior faces of the DCB. This quasi-static loading increases until the first crack starts to grow. At this point, the first crack starts to propagate until reaching 1. When this point is reached, the first fatigue loading stage starts.

Once the fatigue stage (A) is running, the first crack tip reaches the second crack tip; and an unstable crack growth of the first crack tip happens reaching the fatigue stage (B). In order to obtain these crack propagations, a total of 125538 cycles and a crack displacement of around 0.028 mm were used.

After reaching stage (2), a quasi-static loading is imposed on the system until a total displacement of the crack faces of around 0.08 mm. During this stage, the first crack tip surpasses the second one. At that time, the third crack starts to propagate reaching stage(C), where the next fatigue loading stage takes place. Figure 3.4 shows the final stage and location of all of the crack tips during this loading stage.

With this analysis of the multiple delamination benchmark problem, it is shown that the numerical fatigue formulation proposed by [26] is able to capture the cracks tip propagation of multiple delaminations. For this case, further experimental work needs to be done in order to validate the results shown in this chapter.

Parameter study for Weakening patch 4

In the previous chapters, the model proposed by Alfano et al. [28] is considered for further study. This DCB benchmark model is modelled with carbon epoxy-material properties, which is used to enhance the deformation of the beam [20].

A similar study to the one suggested is undertaken in [29], with the change in material properties from a carbon epoxy-material to a glass fiber-reinforce material. Since the properties have changed, the geometry previously described (see Figure 3.1) is modified to better suit the problem.

The various patch implementations previously presented in [20] are examined in [29] utilizing GFRP material. Since the properties and geometry are changed, a numerical and parametrical study of the location and dimensions of the patch is carried out.

The geometrical configuration as well as the patch dimensions obtained from [29] are presented in this chapter. Research on the interface parameters for the crack location is also provided. The main requirements for the manufacturing process of the composite laminate presented in the next chapters are provided in this chapter.

4.1 Patch parameters

In the study presented in [29], a numerical study of the main numerical parameters influencing the simulation results is performed. At first, an estimation of the material properties as well as a mesh sensibility analysis is performed to be able to determine the DCB parameters before including the different patches.

Once the main parameters have been defined, a parametric study of the patches and their locations is carried out. In [29] the incorporation of different types of patches in the DCB was studied. These patches were defined by the augmented onset traction (τ_0) and critical energy release rate (G_c). These parameters provided an overview of the onset of multiple delaminations.

The focus of this thesis is to study the weakening patch configurations. [29] estimates that the properties regarding the weakening patch are the following:

- $\tau_0 = 0$ and $G_c = 0$ of for both mode I and II

The weakening patch does not transfer or carry any weight because it is regarded as a blank gap in the beam. As a result, the weakening patch characteristics are identical to those of the PTFE film. In [29], this material was chosen to generate a weakening patch during the manufacturing process of the composite laminate.

As for the length of the patch, Trabal et al. [20] state that decreasing the patch length reduces the possibility of onsetting multiple propagations. To be able to achieve this phenomenon, the length of the patch should be long enough to initiate and develop multiple delaminations.

In [29], a numerical study was conducted in which the geometry used is shown in Figure 4.3. The main crack is located in the *main interface*, whereas the weakening patch is located 50 mm apart and located in the *secondary interface* with a total length of 50 mm.

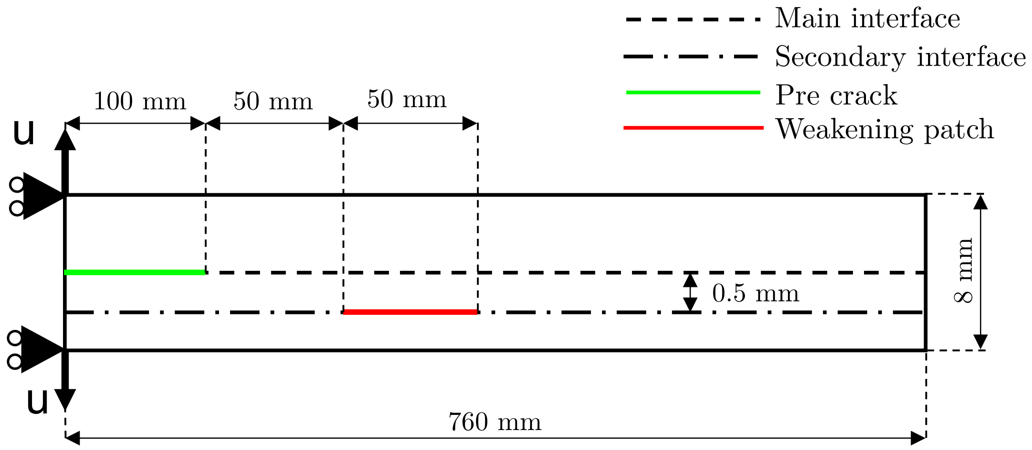

Figure 4.1. Dimensions of the DCB, adapted from [29].

This model was then simulated to determine whether multiple delaminations could be obtained through displacement imposed loading. Figure 4.2 shows the behaviour of the beam for no patch and the weakening patch configurations, as well as the deformation of the beam through this process.

Figure 4.2 shows the deformation behaviour of both DCB configurations. First, a loading stage occurs until the delamination of the crack at the *main interface* propagates. This crack propagates until it reached the weakening patch located at the *second interface.*

In the no patch configuration, the crack continues to propagate without changing its shape. For the weakening patch configuration, it was observed that as the *main interface* crack approached the *second interface* crack, the *second interface* began to delaminate.

This delamination is related to the load drop observed in Figure 4.2. This load drop occurred because of the opening of the weakening patch. After this opening, the DCB was loaded again, without further propagation of the crack fronts.

In this second loading stage, the toughening behaviour of the DCB can be observed, where the load increases as the displacement increases. This toughening behaviour is maintained until a displacement of around 0.065 m is reached. After this displacement, no further toughening effect is seen as the load starts to decrease. This decrease is characterized by the propagation of multiple delaminations. In addition, it was observed that the *main interface* crack stopped propagating, and the main propagation path was located in the *secondary interface*.

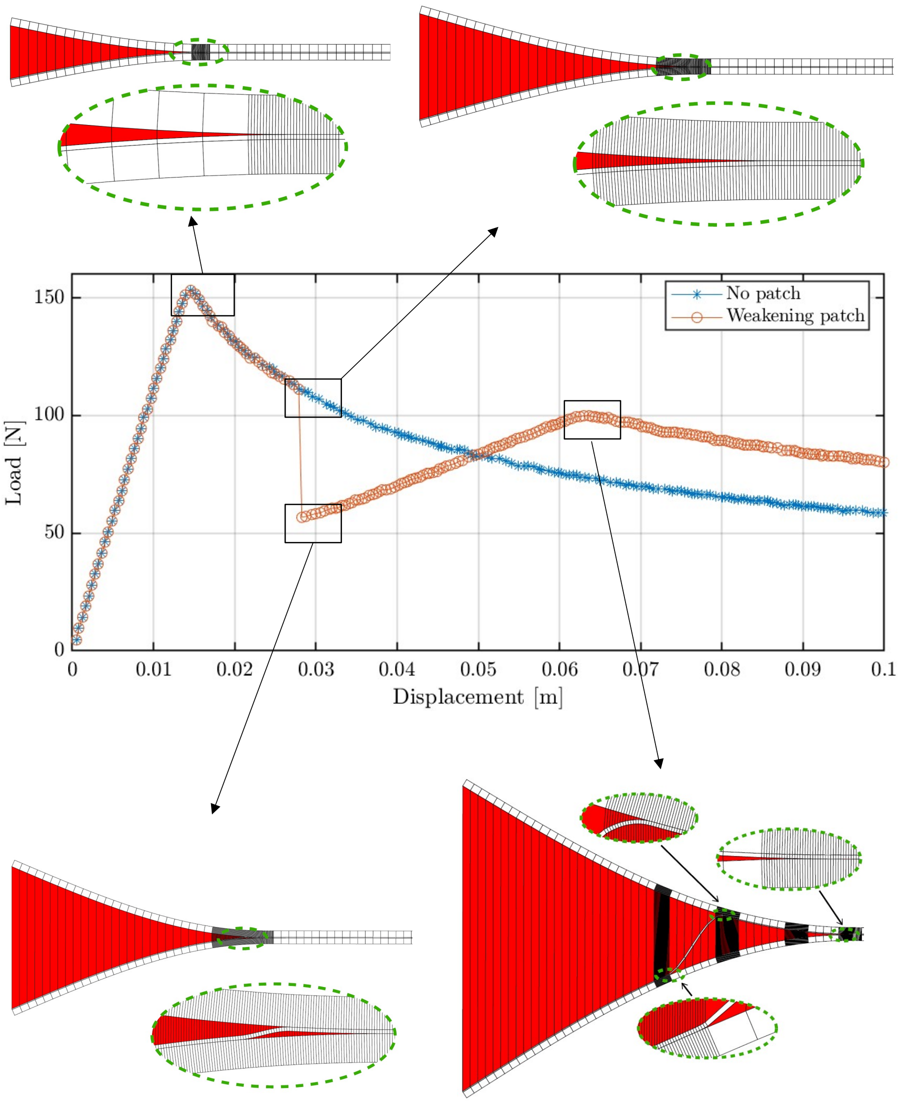

Figure 4.2. DCB equilibrium curve for a virgin and weakening patch configuration. (Adapted from [29])

4.2 Patch length

The length of the patch determines whether multiple delaminations can propagate. The longer the patch, the higher the probability of reaching multiple delaminations. The length of the patch should be enough to ensure that the DCB is sufficiently damaged to be able to develop multiple delaminations [20].

The numerical study shown in Figure 4.2 indicates that a weakening patch with a length of 50 mm is sufficiently long to develop and propagate multiple delaminations. Therefore, this patch length was used for the weakening patch in the manufacturing process.

4.3 Interface location of weakening patch

As previously stated in [29], the material used for the experimental procedure differs from the one presented in [27] and [26]. The material studied in [29] consisted of 16 unidirectional laminates of glass fiber reinforced plastic (GFRP) with an approximate thickness of 0.5 mm.

According to Trabal et al.[20], the closer the weakening patch is to the *main interface*, the more probable it is that numerous delaminations can occur. When determining the position of the weakening patch, special attention must be paid to the placement. If they are placed too close to each other, both interfaces can merge into a single interface.

In [29] a numerical study of the location of the weakening patch interface was performed. It should be noted that the numerical model does not account for phenomena such as fiber bridging and crack jumping.

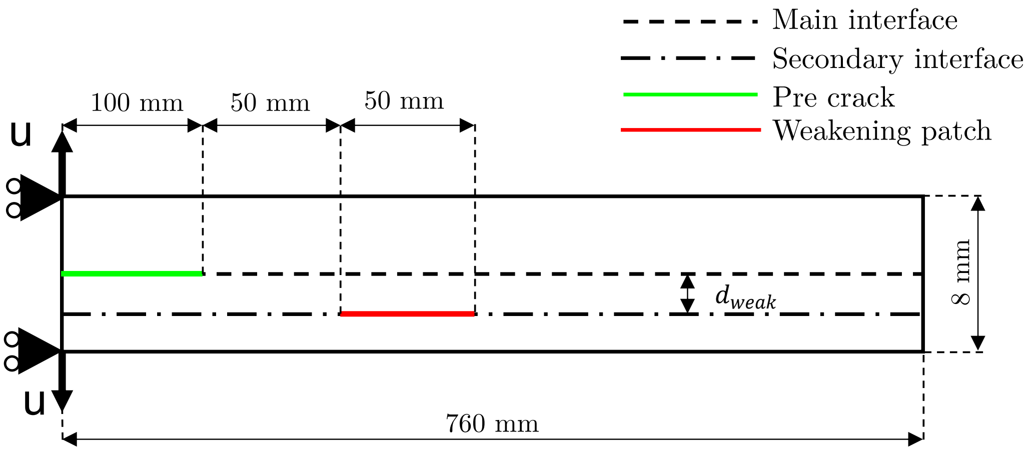

Figure 4.3. Dimensions of the DCB. (Adapted from [29])

Figure 4.3, shows the DCB geometry studied. In this geometry, the parameter d_{weak} is included. d_{weak} is an interface parameter that changes the value to investigate various weakening patch configurations. Only the main and secondary interfaces are simulated in the model studied [29]. The main interface patch and distance between patches are constant parameters.

Figure 4.4 shows the equilibrium curves for different DCB configurations. Similar behaviour with respect to Figure 3.2 can be observed. It can be seen from Figure 4.4 that multiple delaminations are indeed able to propagate in most cases, except for the 2 mm case.

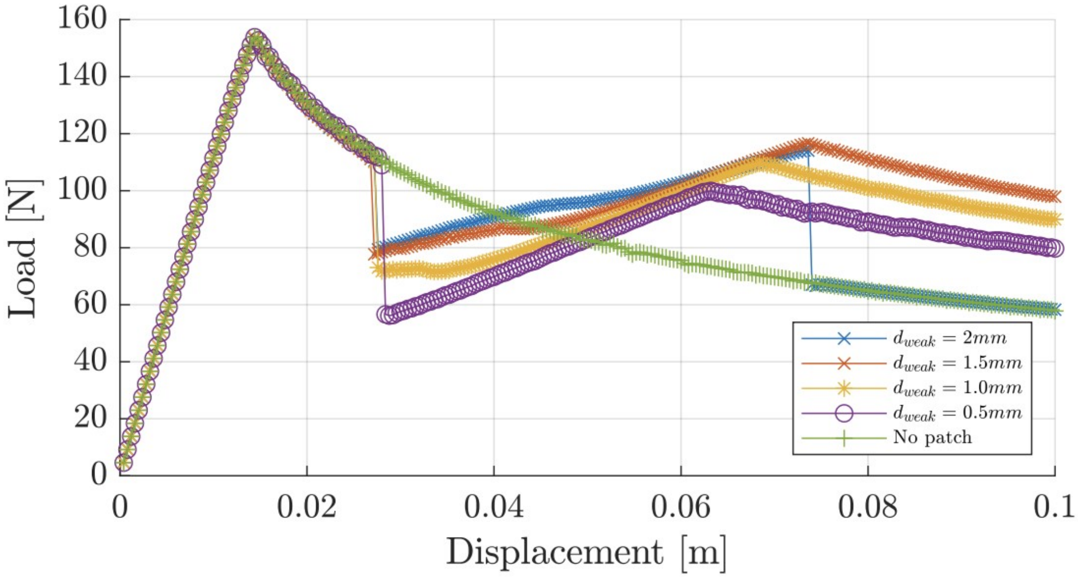

Figure 4.4. Load displacement behaviour for various DCB configurations [29].

In this case, unstable crack growth in the weakening patch was observed as the load increased. In comparison with the other configurations, instead of showing a toughening effect after the second loading stage; a drop in the load axis to the same path as the no-patch configuration was observed. This behaviour indicates that no toughening for the 2 mm configuration is accomplished.

Consequently, a weakening patch can be placed at different interface configurations. It is shown that multiple delaminations are achieved if the *secondary interface* is placed between the three nearest interfaces from the *main interface*.

Experimental Methods and Procedures 5

In the following chapter, an explanation of the experimental procedures used in this thesis is provided. A GFRP composite laminate containing a weakening patch was manufactured to determine whether the behaviour explained in the previous chapters was achieved, and multiple delaminations were obtained.

The test specimens were tested under quasi-static and fatigue loadings using an electrical tensile test machine. The organization of the chapter is as follows: First, the manufacturing process and test setup are explained. Subsequently, preliminary test experiments on quasi-static loading are introduced, followed by an explanation of the fatigue test procedure.

5.1 Manufacturing process

The manufacturing process of the DCB specimen was performed to validate the results presented in Section 4. It should be noted that the manufactured material has the same properties as those presented in Chapter 4.

The manufactured material consisted of 16 unidirectional non-crimp fabric glass fiber mats ($\pm 80 and 0$) with an areal density of 800 g/m^2 infused with PRO-SET INF114-INF212 standard infusion epoxy [30]. The layup is symmetric concerning the center plane where the unidirectional layers face the mid-plane and two pre-cracks are induced in the material, one in the mid-plane and the other between the sixth and seventh layers.

To create the two pre-cracks as previously shown in Figure **??**, a 13 μm thick PTEE film is used. Figure 5.1 shows the location of the two pre-cracks during the layup of the laminae. These patches are introduced to induce multiple cracks in the material, making it easier to promote multiple delaminations.

After the pre-cracks were located and all the layers were stacked, vacuum-assisted resin transfer moulding (VARTM) was used. Subsequently, a curating process was used in accordance with the resin manufacturer specifications.

(a) Precrack location

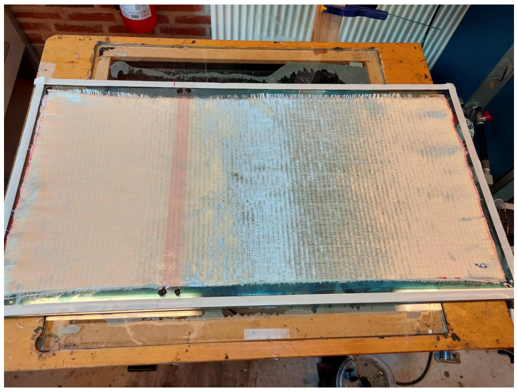

(b) Weakening patch location

Figure 5.1. Pre-crack locations during the manufacturing process.

The initially created plate has a total dimension of 950 × 450 mm. However, the borders of the plate need to be removed due to the impurities of the plate, remaining with a plate of dimensions 380 × 870 mm. Afterwards, the plate was cut into 12 specimens with dimensions of 30 × 870 mm as shown in Figure 5.2.

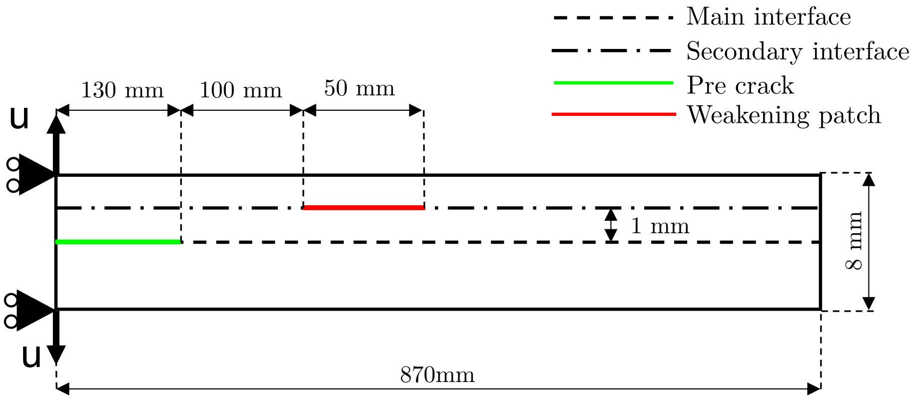

Figure 5.2. Configuration of the manufactured test specimens.

After the 12 specimens were manufactured and to attach the specimen to the testing machine, four holes were drilled in the specimen. These drilled holes were placed at a distance that resulted in a precrack length of 50 mm according to the ASTM standards for mode I fracture toughness characterization [17].

5.2 Test setup

Now that the DCB has been manufactured, various tests are performed to study if a toughening behaviour can be achieved through multiple delaminations. For doing this, a tensile testing machine is used. An image of the experimental test setup is shown in Figure 5.3. The main components of the test are:

- Tensile test machine (Electropuls E10000)
- GFRP DCB specimen

- Two Light sources
- Camera
- Hinge fixture

In order to set up the experiment, some adjustments need to be made to the machine to perform the fatigue test. These adjustments relate to the mounting parts of the machine, where a 2 kN load cell is attached to the lower part of the tensile testing machine. An extension arm is also fitted to the upper part to provide the correct range of movement to carry out the tests.

After fixing the load cell and gripper onto the machine, a hinged fixture is attached to both ends for holding the specimen. These hinges provide a flexible range for the fatigue loading test placing the rotational axis of the hinged at the neutral line of each beam arm of the specimen [31].

Once the DCB is placed in the machine, an external computer is used to track the pictures taken by the camera. The camera is a FLIR Blackfly CCD camera (2448 × 2048 pixels, monochrome) and it is the one that is used to acquire images of the specimen during the loading tests. Since the distance from the DCB to the camera is not enough to catch any DCB feature, the specimen is illuminated by two LED white light sources (NILA Zaila Daylight spotlights). These leds provide enough light for the camera to be able to take high-resolution pictures during the different loading stages.

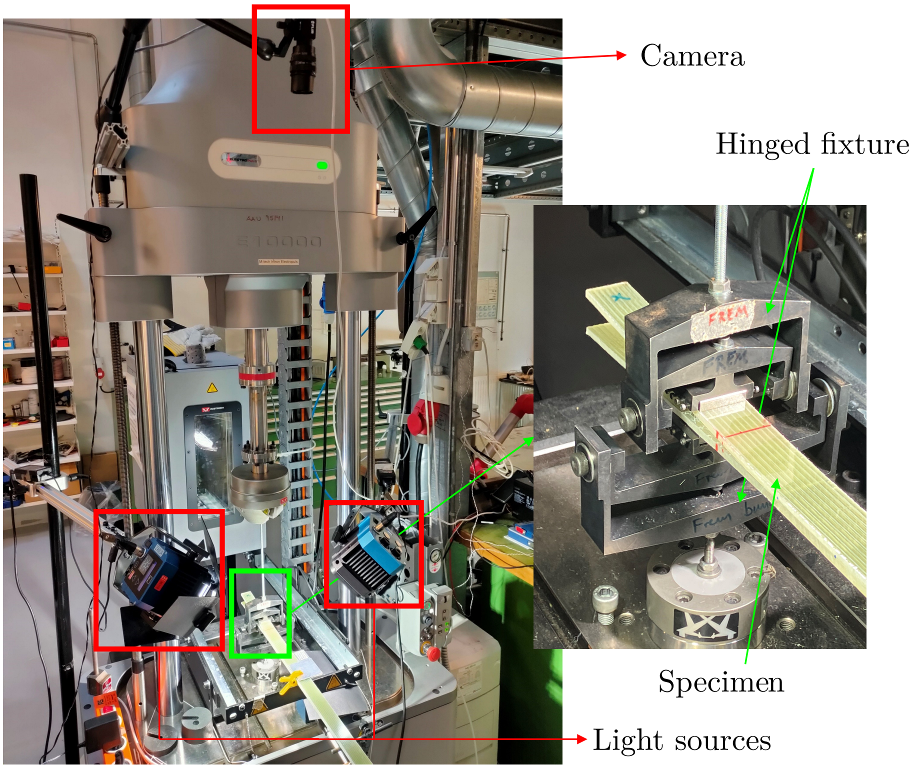

Figure 5.3. Lab setup.

5.3 Preliminary test experiment

In order to get to know the material behaviour and the testing machine, preliminary experiments do take place to see if the testing conditions are enough to propagate multiple delaminations and to see if there is any correspondence with the data shown in previous chapters. The layup and geometry of the specimen used are shown in Figure 5.2.

The preliminary test consists mainly of a quasi-static loading test, in which the camera attached to the tensile machine is taking pictures to relate the loading stage with the delamination propagation. Figure 5.4 details the quasi-static loading stage procedure.

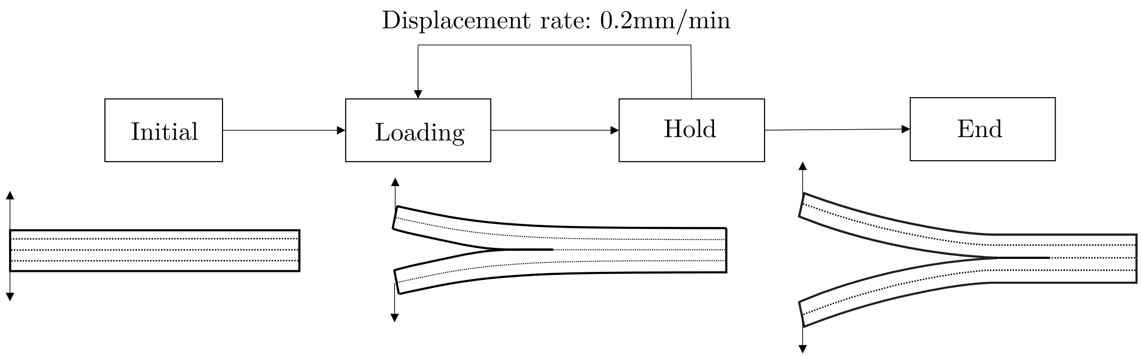

Figure 5.4. Quasi-static loading procedure.

The quasi-static loading stage started from the initial position, where the beam was unloaded and the specimen was intact. Subsequently, a loop containing two blocks was initiated. In the first block a displacement rate of 0.2 mm/min was applied, followed by a hold block where the loading stopped for 2 seconds, in which a photograph of the specimen was taken. This loop was repeated for a certain number of cycles until the end block was reached.

Some machine limitations that could affect the test results should be noted. For example, the maximum displacement range between both hinged fixtures was approximately 60 mm.

5.4 Fatigue test procedure

As mentioned in Chapter 4, a novel fatigue loading study of a DCB was performed numerically by [27]. Since no further experimental work has been conducted in this field, this thesis attempts to replicate these studies experimentally.

Figure 3.3 shows that the fatigue test performed in [27] consisted of four different stages. This load spectrum was then adapted to better suit the experimental test developed in this study. Figure 5.5 depicts the fatigue test configuration used in the experimental fatigue testing.

Figure 5.5 shows the displacement-time graphs together with the expected specimen behaviour. It can be observed that 4 different stages are analyzed, two quasi-static and two fatigue loading stages. The two fatigue stages are characterized by crack propagation occurring during these stages.

The fatigue stages were divided into two categories. The first stage is the fatigue loading stage, which is considered a low-amplitude load level. The second is a high-amplitude load level. These fatigue studies are considered variable amplitude test.

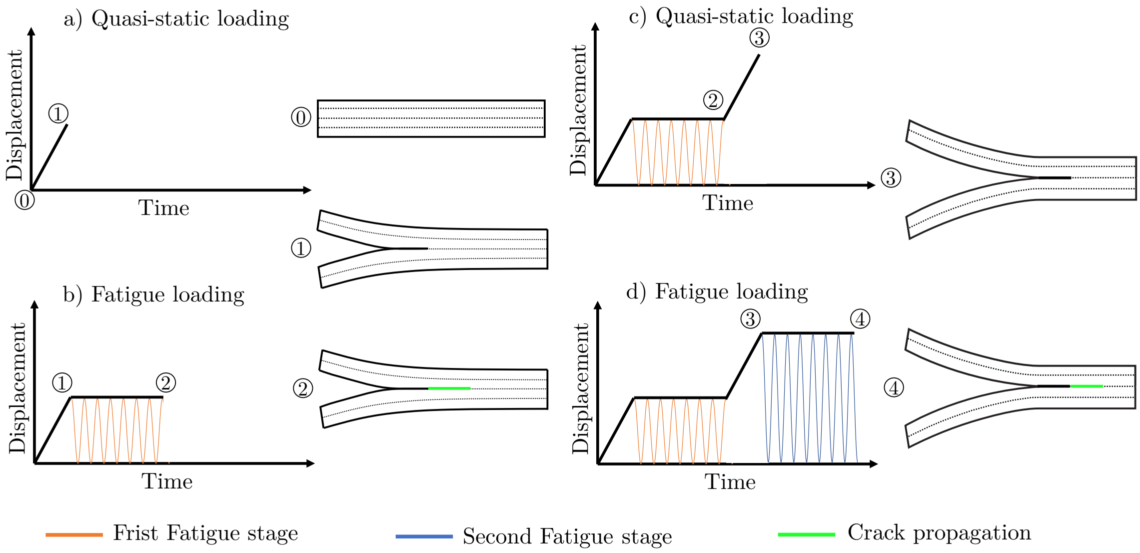

Figure 5.5. Fatigue test load spectrum and specimen behaviour.

The fatigue stages are characterized by different parameters which need to be defined before testing. These parameters are the amplitude, number of cycles, maximum and minimum displacements, and frequency.

The amplitude is calculated as shown in Eq. 5.1. The fatigue stages start at the maximum displacement, which is reached at the end of the previous quasi-static stages.

$$Amplitude = \frac{\Delta d_{max} - \Delta d_{min}}{2} \tag{5.1}$$

All tests were carried out in pure mode I at a constant minimum-to-maximum ratio of applied displacement of $R_\delta = \delta_{min}/\delta_{max} = 0.1$. Also, a small deflection regime to control the deflections of $\delta/a < 0.4$ is used according to ASTM D5528-01 [17].

6 Results and discussions

In this chapter, the different results obtained through the quasi-static and fatigue loading tests will be presented. As the main focus is to study the toughness of the specimen by promoting multiple delaminations, the equilibrium curve is plotted as well as some visual inspection of the specimen delamination.

6.1 Quasi-static loading

As mentioned in the previous chapter, a quasi-static loading case is first carried out. The purpose of this test is to know the behaviour of the material under these test conditions. Also, this test is used to study if multiple delaminations are achieved. For this, the load-displacement graph is analyzed. Figure 6.1 shows the different equilibrium curves for the experimental test and for the analytical solution.

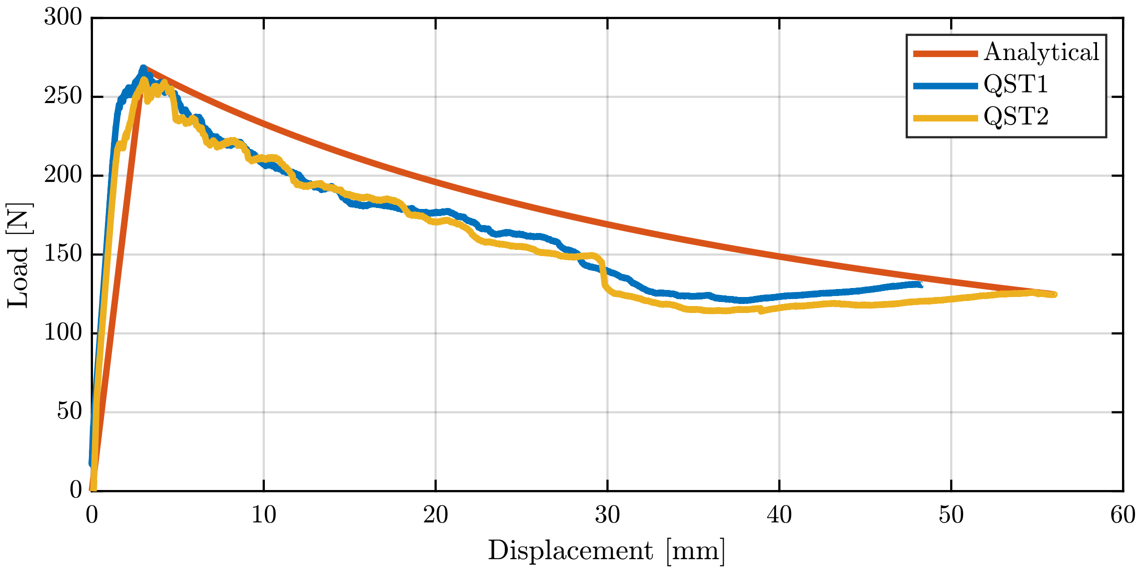

Figure 6.1. Equilibrium curve for two quasi-static states and the analytical solution.

It can be observed from the results obtained the similarity between the experimental and the analytical results. For the analytical solution, a higher load is required during the crack propagation. In the test specimens, it can be possible that multiple material defects could be created in the specimen during the manufacturing procedure.

Also, it can be observed that no unstable crack growth happens in the tested specimens in comparison to the obtained in [29]. This is because the delamination phenomena are constantly occurring during the loading stage. This delamination process is shown in Figure 6.2.

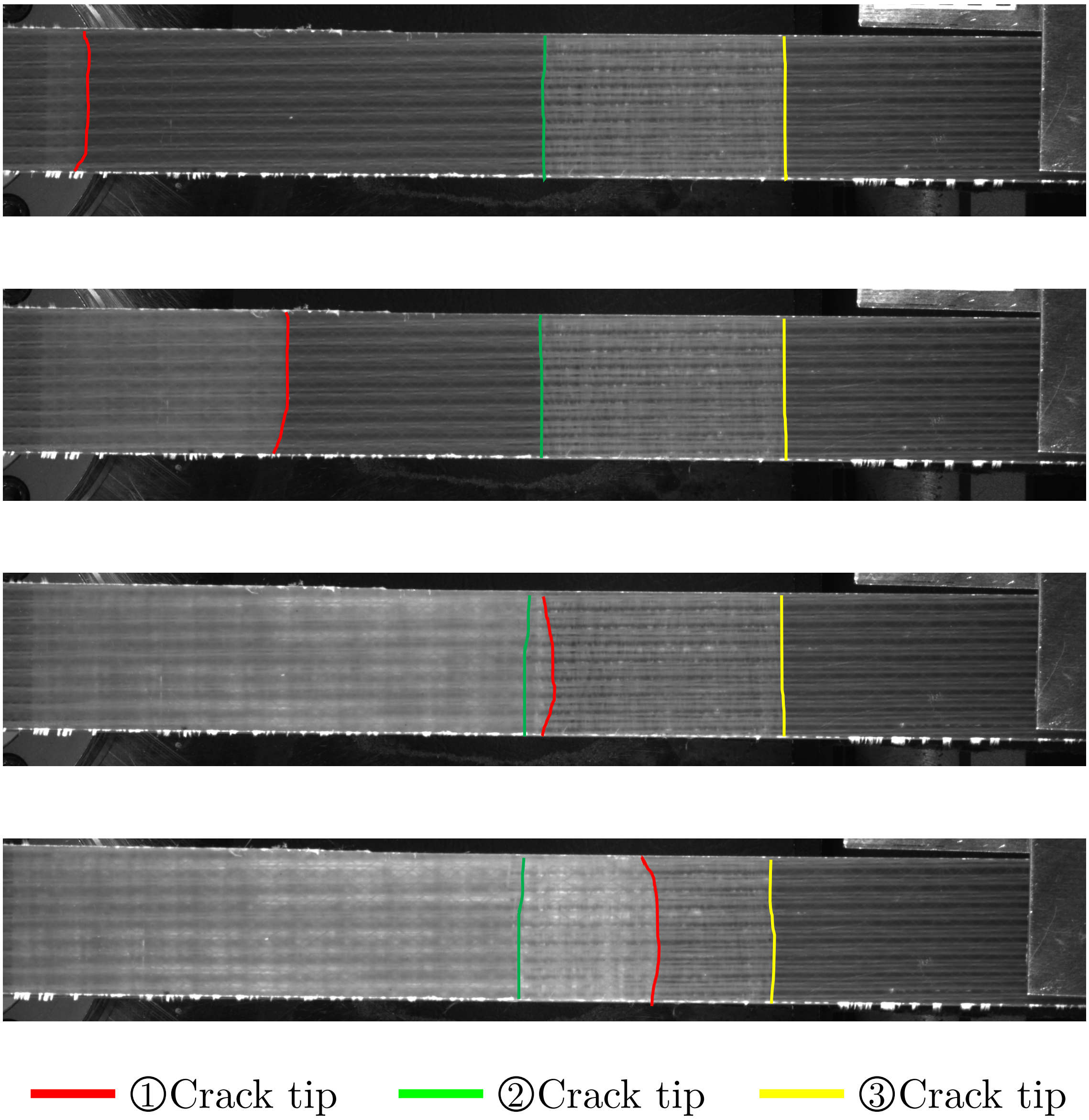

Figure 6.2. Crack tips propagations of the quasi-static loading specimens.

It can be seen a clear delamination of the C. tip ① . For C. tip ② and C. tip ③ delamination is barely noticable. This is due to the machine displacement range. From this result, it was concluded that new holes needed to be drilled in the specimen to be able to see if multiple delaminations are achieved under quasi-static loading.

6.2 Modified mounted holes configuration

Since no delamination is observable using the previous configuration, it is decided to move the drilled holes forward in the specimen, to shorten the distance between the drilled holes and the weakening patch. Figure 6.3 shows the new configuration.

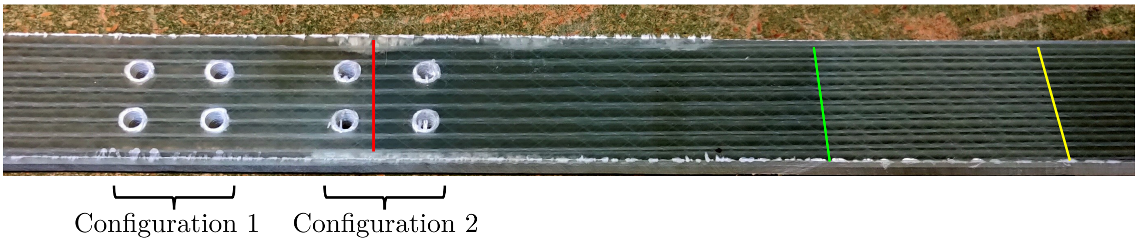

Figure 6.3. Modified configuration.

Figure 6.3 shows that the ① crack tip is located in between the holes of the second configuration. This crack location does not meet the ASTM D5528-01 standards [17] since the crack tip should be located 50 mm away from the holes.

To meet these standards, the crack is propagated until it reaches a distance of 50 mm from the second configuration. This change was made for the remaining specimens as shown in Figure 6.4.

Figure 6.4. Modified pre crack configuration for the four tested specimens.

From the remaining specimens, two quasi-static loading tests and two fatigue loading tests are performed to study the toughening behaviour of the material due to multiple delaminations.

6.3 Quasi-static loading for modified configuration

Once the modification of the mounting holes and the pre crack is made, a quasi-static loading case is done to see if multiple delaminations are obtained through this test and to study how the material would behave with this parameter modification.

Figure 6.5 shows the material behaviour of a load-displacement graph. The cases for the new configurations and the results obtained from the previous test are shown.

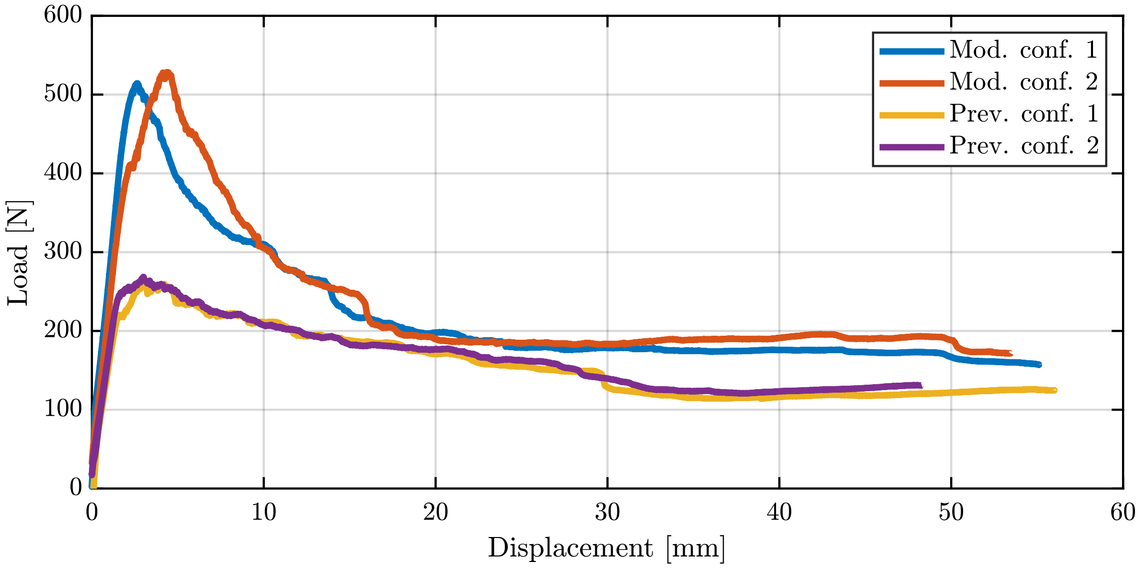

Figure 6.5. Quasi-static loading comparison between the new and previous configuration.

It can be observed from Figure 6.5 that the load resistance has increased for the modified configuration, making the load necessary to propagate the crack around 500 N. In this modified configuration, a constant load range is obtained through the whole propagation of this patch is observed.

Figure 6.6 shows the different crack tips behaviour during the quasi-static loading stage presented in Figure 6.5. For C. tip ① represented in red, it can be seen how it propagates through the main interface until eventually reaching the weakening patch.

After C. tip ① surpasses C. tip ②, a small delamination of C. tip ② can be observable. After this moment, is observed that C. tip ② remains static and does not continue to propagate further.

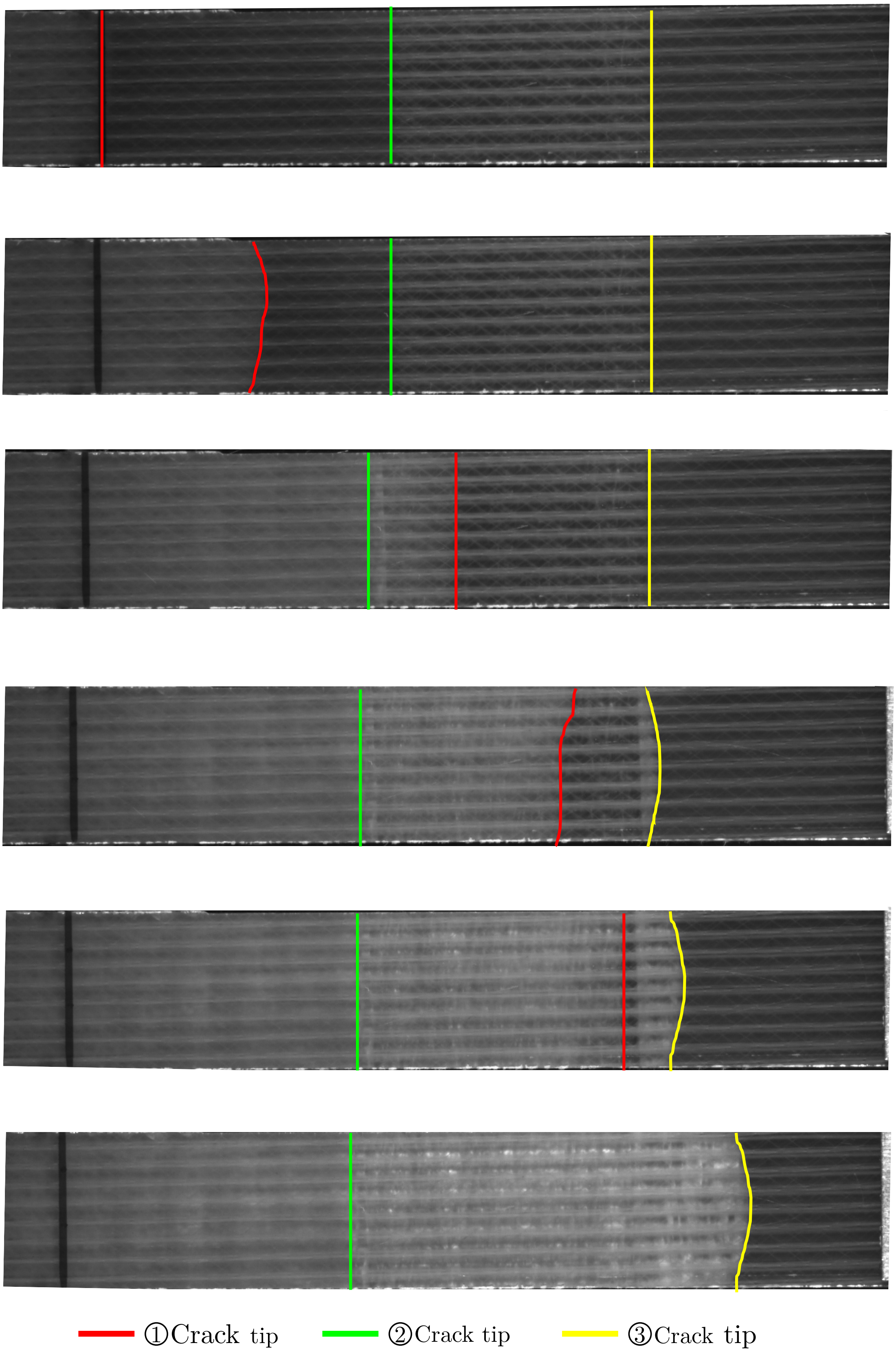

Figure 6.6. Crack tips propagation during the fatigue test.

After surpassing ②, ① continues to propagate. While ① stills propagates through the weakening patch, ③ crack tip starts to propagate. Once ① reaches ③, no further information of ① can be obtained through the camera since the weakening patch is located two interfaces above the interface containing ①.

6.4 Fatigue test loading

After observing the possibility of achieving multiple delaminations under quasi-static loading conditions, a fatigue test was conducted to determine whether multiple delaminations can also occur under these specific test conditions.

Before implementing fatigue testing, some parameters, such as the displacements in which the fatigue loading steps start, need to be first determined. From Figure 6.7 it can be observed that two main fatigue stages were used.

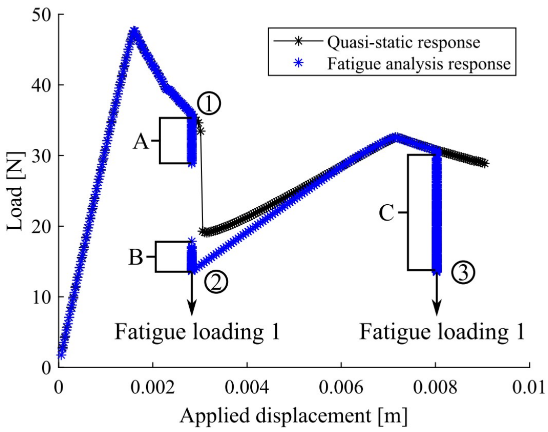

Figure 6.7. Fatigue and Quasi-static equilibrium curves [27].

The first fatigue stage started when C. tip ① started to propagate entering fatigue block A. While block A is running, an unstable C. tip ① delamination growth occurs, jumping to block B. The second fatigue stage occurs after the C. tip ③, which belongs to the weakening patch, begins to propagate.

The focus of this work is to investigate the response of the beam by propagating delaminations under fatigue loading. First, the fatigue behaviour after ① initially started propagating is studied. Second, another fatigue loading stage takes place when ① has reached the weakening patch and has surpassed ② but has not reached ③ yet. The purpose is to observe the material behaviour and determine if there is an observable toughening effect in the specimen. Figure 6.8 shows the location of the different crack tips.

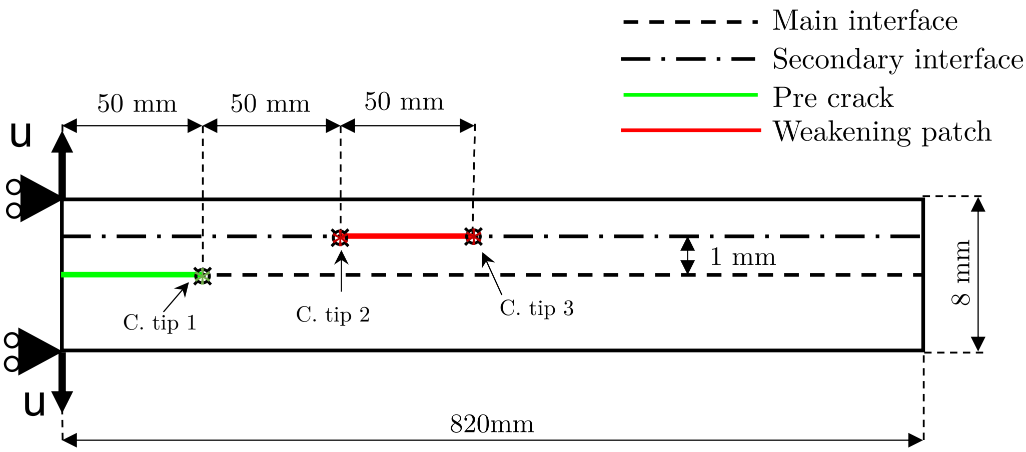

Figure 6.8. DCB geometry showing the location of the different C.tips.

The fatigue test is displacement-driven, meaning that the displacement thresholds for the different fatigue stages need to be defined before performing the test. To define these thresholds based on the previous assumption, a visual inspection of the different pictures taken during the quasi-static case is done.

The analysis involved a visual inspection of the positions of different crack tips during the quasi-static test. Each image data was matched with the equilibrium curve to precisely determine the position of the propagation of each crack tip. The parameters obtained from this analysis are presented in Table 6.1, where the amplitude can be calculated through Equation 5.1.

Table 6.1. Fatigue test parameters.

Specimen	Stage	δ_{min} [mm]	δ_{max} [mm]	Displacement rate [mm/min]	f [Hz]	Cycles	Cycle loops
Fatigue test 1	Quasi-static	0	7.2	0.2	-		
	Fatigue LA	0.72	7.2	-	3	100	1500
	Quasi-static	7.2	32.2	0.2	-		
	Fatigue HA	3.22	32.2	-	2	100	1500
Fatigue test 2	Quasi-static	0	7.2	0.2	-		
	Fatigue LA	0.72	7.2	-	3	100	3000
	Quasi-static	7.2	32.2	0.2	-		
	Fatigue HA	3.22	32.2	-	2	100	3000

Two different specimens are used for fatigue testing, which is separated into fatigue test 1 (FT1) and fatigue test 2 (FT2). Even though the displacement and frequency parameters are the same in both tests, the number of cycles is changed to study the crack propagation and the material response under different numbers of cycles.

Now that the fatigue parameters have been defined, the test can be performed. Figure 6.9 shows the different fatigue test data obtained. Also, the quasi-static loading stage is plotted to see if any toughening effect is observable from this test.

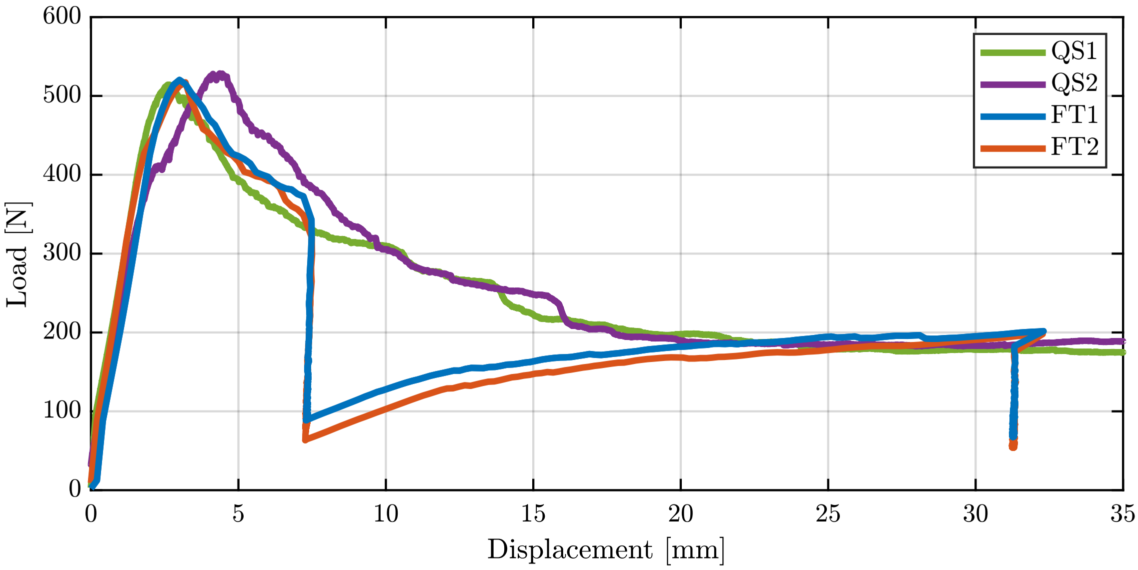

Figure 6.9. Fatigue test results compared to quasi-static cases.

Figure 6.9 displays the fatigue and quasi-static response of the DCB. During the loading phase, a similar behaviour to what is observed in the quasi-static analysis is shown. Upon reaching the first fatigue loading stage, there is a decrease in load from approximately 390 N to nearly 90 N. Following this stage, another loading stage occurs, where some toughening behaviour can be observed towards the end. Before reaching the second fatigue stage, irregular data is noticed due to the displacement exceeding the limit. However, it stabilizes demonstrating a behaviour similar to the first stage.

Concerning the difference between the number of cycles for both specimens, it can be seen that in the first fatigue stage, the FT2 specimen reached a lower load compared to the one reached by the FT1 specimen. In the following loading stage, it can be seen that although both specimens start this stage at different load levels, at the end of this loading stage, both reached the same load value of around 200 N. For the final fatigue test, is observed that both specimens show some irregular data gathered from the test in which a displacement bigger than the limit is achieved. At the final stage, it is observed that both cracks almost reach the same load level, but the one reached by the FT2 specimen is around 10% lower.

As stated before, a camera is attached to the testing machine which is taking pictures of every loading cycle, resulting in a picture taken every 100 cycles. From these pictures, the different crack tip propagations can be observed, as shown in Figure 6.2 and Figure 6.6. By analyzing these images, it becomes possible to measure the propagation of the crack tips.

This measurement is done for the fatigue loading stages, where the propagation distance is measured every 30000 cycles. From Figure 6.2 and Figure 6.6 it can be seen that at certain point, ① and ③ become indistinguishable. For this case, it is assumed that both cracks propagate the same distance.

After a certain displacement, when ① and ③ become indistinguishable, the measurement data of the propagation of ① and ③ is not accessible due to a misplacement of the reference pattern holder. For this case, the last propagation data point is measured once the specimens have completed the test.

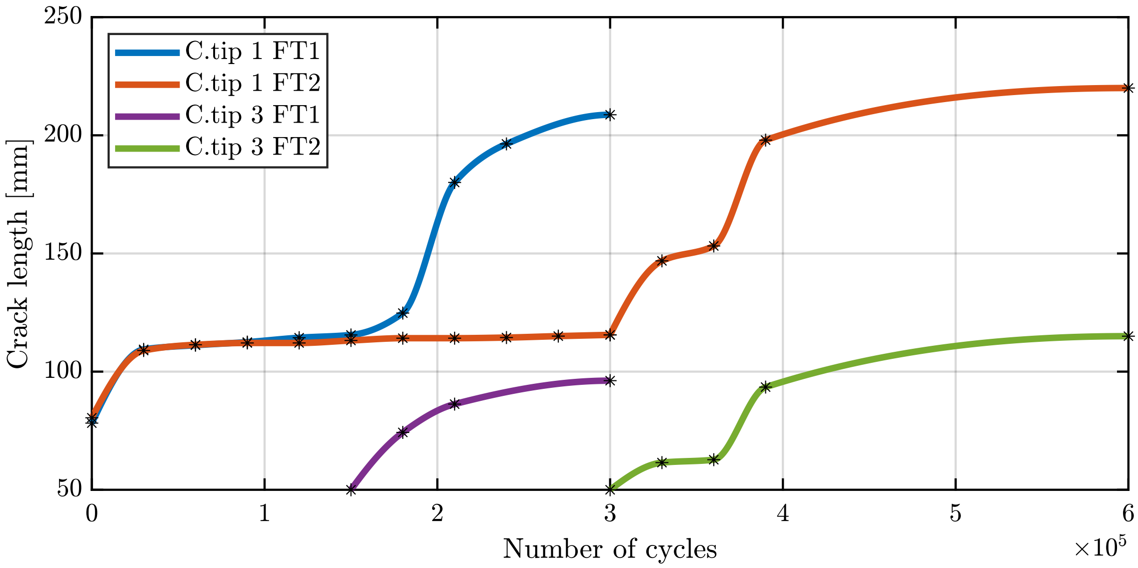

Figure 6.10. Crack length during the fatigue loading stage.

Figure 6.10 shows the increase in the length of the different cracks with the number of cycles. In the case of FT1, the crack length increases until a total amount of 300000 cycles, a total of 150000 cycles for each fatigue stage. For the FT3 case, it can be seen that more data is obtained through the first fatigue stage. However, the second stage does not provide much data. Fro this analysis, C.tip ② in neglected. To complete this data, a cubic interpolation is employed.

For this analysis shown in Figure 6.10, each crack is assumed independent from the other, meaning that each crack is treated separately. However, the data associated with crack propagation is used in the following manner:

- For the first fatigue loading, the data of C. tip 1 is employed.
- At the beginning of the second fatigue loading and after the quasi-static stage, C. tip 1 is measured again, while C. tip 3 has not yet propagated.
- The measurement of C. tip 1 is then connected to the measurement taken at the final of the first fatigue stage. The data from this point is then analyzed in relation to the second fatigue stage.
- Once C. tip 3 starts to propagate, is measured and is only analyzed with the second fatigue data.

This approach ensures that each crack is examined individually while utilizing the appropriate data from different stages of the fatigue testing process.

Now that the crack length for the different crack tips is obtained, it can be studied its relation to the crack growth rate to see how the different cracks behave as shown in Figure 6.11.

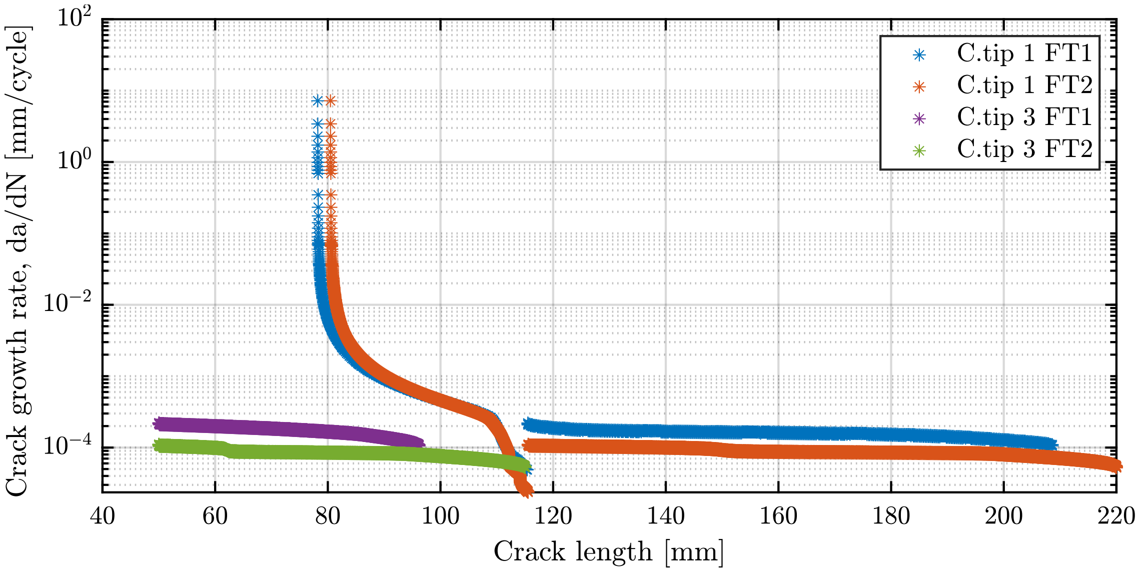

Figure 6.11. Crack growth rate with respect to the number of cycles.

Based on the data presented in Figure 6.11, notable observations can be made regarding the crack growth rates. For C.tip 1 a jump in the crack growth rate around 120 mm is observed. This phenomenon is attributed to the transition in amplitude levels during the test. It has been noted that when transitioning from a low amplitude to a high amplitude, a sudden increase in the crack growth rate occurs for the specific amplitude change [32].

On the other hand, for C. tip 3, a more consistent and steady increase in crack length can be observed. This behaviour can be attributed to the difference in the number of cycles, where in the first fatigue stage the higher number of cycles results in a relatively higher crack growth rate compared to the second fatigue stage.

Based on what is stated in Section 1.5, for the fatigue characterization, the SIF calculation must be discarded and it should be characterized in terms of the energy release rate (SERR). The SEER can be calculated using Eq.6.1. For this calculation, the specimen is assumed to be perfectly clamped and the specimen material is considered isotropic [24], [32].

$$G_I = \frac{2P\delta}{2wa} \tag{6.1}$$

Where P denotes the reaction force, δ denotes the applied crack tip displacement, a denotes the crack length, and w denotes the width of the sample.

The SERR in Eq.6.1 is based on a pure mode I opening and is computed based on the beam theory. Based on the work of Sørensen et al.[33], Eq.6.1 is theoretically admissible under a small damage process zone. Ignoring that the large-scale damage zone influence is consistent with the results of previous studies on fatigue-driven delamination, a small damage process zone is considered [33].

Since the fatigue test is considered a displacement control test, Eq.6.1 can be rewritten in terms of the displacements shown in Eq.6.2.

$$G = \frac{9E_{11}I}{4wa^4}(\delta)^2 \tag{6.2}$$

This equation considers the young modulus E_{11} and the second moment of inertia I as well as the crack length a and the imposed displacement δ. In the literature, delamination due to fatigue is characterized by the maximum SERR (G_{max}) or SEER range as ($G_{max}-G_{min}$) or $(\Delta\sqrt{G})^2$. The term used in Eq.6.3 can be seen as an analogy of the term used in fracture mechanics [34]. Where G_{max} stands for the maximum energy released rate while G_{min} stands for the minimum.

$$(\Delta\sqrt{G})^2 = (\sqrt{G_{max}} - \sqrt{G_{min}})^2 \tag{6.3}$$

Now, a study of how the SERR is related to the fatigue loading test is conducted. First, it is studying how the SERR change concerning the cycles, to see whether there exists a toughening in the whole structure.

This study is done individually. An analysis of the first crack tip SERR is made for both fatigue testing cases (FT1 and FT2). This is done to study the influence that the propagation of both of the crack tips has on the total toughness of the structure. Figure 6.12 shows how the normalized SERR changes with the number of cycles for C.tip ① .

The graph shows that at the start of the fatigue loading stage, the normalized SERR is around 0.1, which makes sense since the crack during the first fatigue loading stage is already propagated. A later increase can be observed, which corresponds to the C.tip 1 reaching the weakening patch. Afterwards, it makes the SERR decrease again.

For the second fatigue loading stage, it can be seen that the SERR increases until a value of 0.7 is reached. This means that after the quasi-static loading stage, the crack needs more energy to propagate for this stage than for the previous one, achieving a toughening behaviour. After the initiation of this stage, it can be seen that the SERR decreases, meaning that the crack is propagating. The SERR behaviour for C.tip ③ is shown in Figure 6.13.

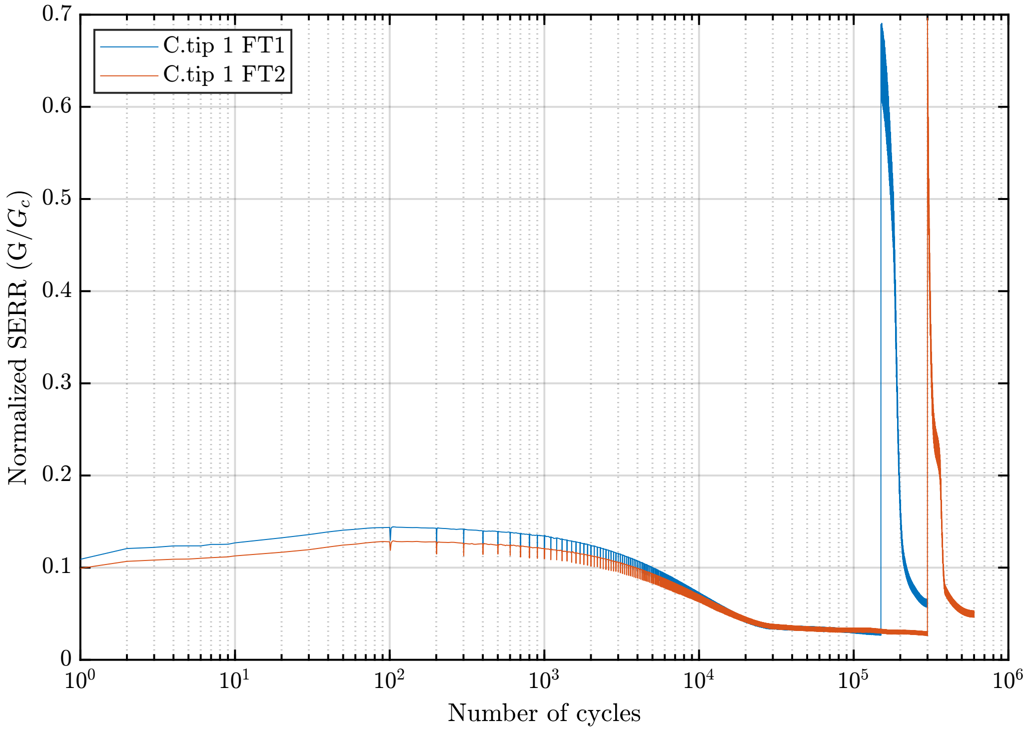

Figure 6.12. Change of the normalized SERR with the number of cycles for C.tip ①.

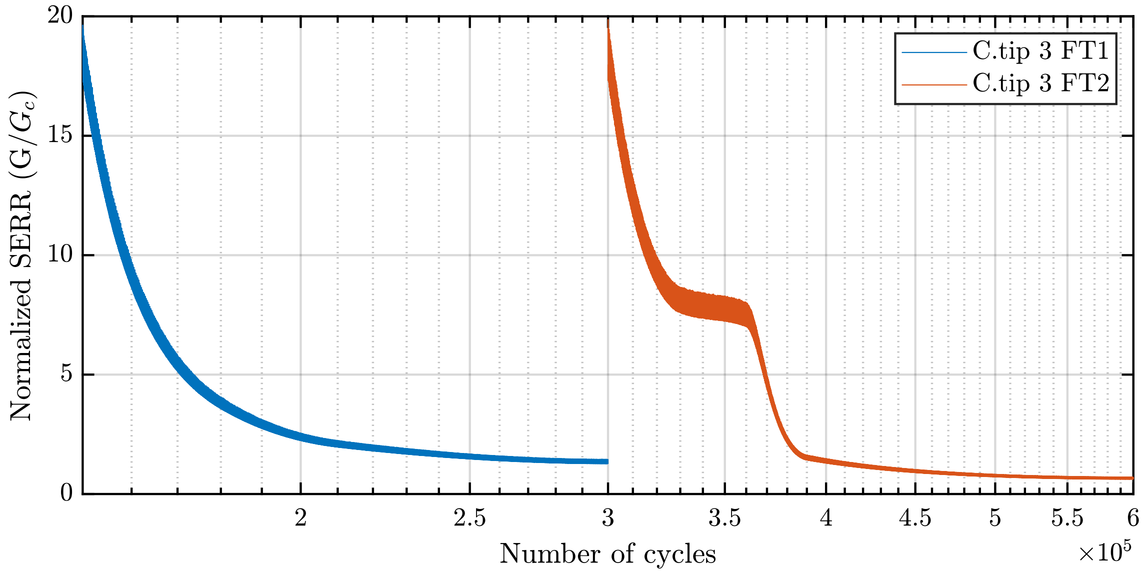

Figure 6.13. Change of the normalized SERR with the number of cycles for C.tip ③.

This graph shows the different behaviour for the C.tip ③ for the different fatigue stages. It can be seen that the shape of the FT2 is different from the FT1, which could account for the different shape from the crack growth shown in Figure 6.10. Concerning the SERR behaviour, it is observed that at the start of the fatigue stage, to make C.tip ③ propagate, the normalized SEER has to have a greater value than the one needed to propagate C.tip ① in FT3.

In order to complete the study, the different crack tip propagations can also be represented in terms of the crack growth rate and the SERR. Figure 6.14 shows a similar result to the one obtained in Figure 6.11. This is introduced in order to complete the study.

The logarithmic graph (see Figure6.14) shows the behaviour of the different crack tips in terms of the crack growth rate and SERR. C.tip ① shows similar behaviour in FT1 and FT2, which corresponds to what has been analyzed in this chapter. For the second fatigue stage, a jump can be observed, where the data for FT2 is in a lower position with respect to FT1 due to the number of cycles. The same behaviour can be seen for C.tip ③ FT1 and FT2, where a higher SERR value is achieved from C.tip ③ as shown previously.

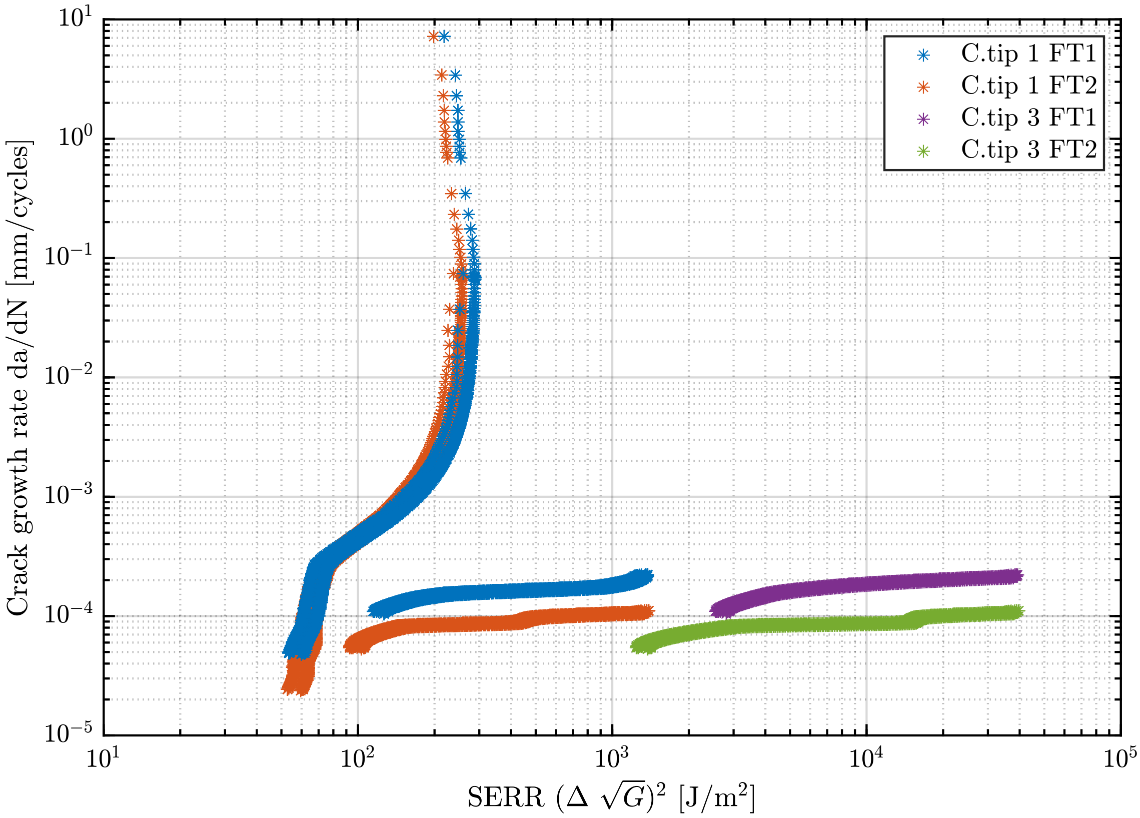

Figure 6.14. Crack growth rate change with respect to SERR.

7 Conclusion

The aim of this thesis was to study and characterize multiple delaminations through fatigue driven test, to see if a toughening behaviour could be observed through experimental testing based on the numerical formulation proposed by Trabal et al .[27].

To follow this path, a parameter study based on [29] has been conducted to determine the geometry of the required specimens. Subsequently, a GFRP composite laminate containing an initial pre-crack and a weakening patch has been manufactured. The laminate was then divided into 12 tested specimens.

Once the specimens were manufactured, preliminary quasi-static loading tests has been carried out to observe the behaviour of the material. After this preliminary test, the pre-crack configuration has been modified based on the data obtained.

After this modification, two quasi-static tests have been performed in which multiple delaminations were achieved. These quasi-static cases have been also used to determine the main parameters used in the fatigue-driven tests.

From the equilibrium curve obtained from the fatigue test, a toughening behaviour can be observed between the fatigue stages. This material toughening provides a first insight into the main focus of this thesis, which is based on the toughening of the material by promoting multiple delaminations.

After observing this toughening behaviour in the test, fatigue characterisation is performed by calculating and representing various parameters such as crack growth rate and strain energy release rate with respect to the number of cycles.

Overall, this thesis proposed a novel study which considers the performance improvement of composite materials by promoting multiple delaminations under fatigue-driven loading conditions. Thus, this thesis contributes to the state-of-the-art by providing this work as a benchmark case for further studies in this field.

7.1 Further work

Based on the finding made in this study, further development is suggested:

More accurate crack measure procedures. A more accurate crack measure procedure should be developed to be able to study past the crack merging of C.tip ① and c.tip ③. To see and distinguish the individual crack growths.

Further testing. Based on ASTM D5528-01 standards at least five specimens should be considered per test condition [17].

Precise calculation of the strain energy released rate. A more precise and concise calculation of the SERR should be develope to be able to fully calculate this parameter.

Bibliography

[1] Robert M Jones and Robert Millard. *Mechanics of composite materials- Second edition*. Tech. rep. 1999.

[2] PK Mallick. “Fiber Reinforced Composites Materials, Manufacturing, and Design”. In: ().

[3] Daniel F.O. Braga et al. *Advanced design for lightweight structures: Review and prospects*. 2014. DOI: 10.1016/j.paerosci.2014.03.003.

[4] Christian Boller and Matthias Buderath. *Fatigue in aerostructures*. Feb. 2007. DOI: 10.1098/rsta.2006.1924.

[5] M. McGugan et al. “Damage tolerance and structural monitoring for wind turbine blades”. In: *Philosophical Transactions of the Royal Society A: Mathematical, Physical and Engineering Sciences* 373.2035 (Feb. 2015). ISSN: 1364503X. DOI: 10.1098/RSTA.2014.0077.

[6] W Hwang, KS Han - Journal of Composite Materials, and undefined 1986. “Fatigue of composites—fatigue modulus concept and life prediction”. In: *journals.sagepub.com* (). URL: https://journals.sagepub.com/doi/pdf/10.1177/002199838602000203.

[7] Hassan Ijaz et al. “Fatigue delamination crack growth in GFRP composite laminates: Mathematical modelling and FE simulation”. In: *International Journal of Aerospace Engineering* 2018 (2018). ISSN: 16875974. DOI: 10.1155/2018/2081785.

[8] Vinay K Goyal et al. *Analytical Modeling of the Mechanics of Nucleation and Growth of Cracks*. Tech. rep. 2002.

[9] J Zhang. “Characterization and analysis of delamination fracture and nanocreep properties in carbon epoxy composites manufactured by different processes”. In: *journals.sagepub.com* 40.14 (July 2006), pp. 1287–1299. DOI: 10.1177/0021998305057438. URL: https://journals.sagepub.com/doi/pdf/10.1177/0021998305057438?casa_token=opr7uuYVG_QAAAAA:5Cl5hR4-3SB7uzpwRAW4YmUzV9halxPvodP5EiS8u56qP7RnEty8XrkxTI1WwYjsdb7gNW0SlBnE.

[10] TE Tay - Appl. Mech. Rev. and undefined 2003. “Characterization and analysis of delamination fracture in composites: an overview of developments from 1990 to 2001”. In: *asmedigitalcollection.asme.org* (). URL: https://asmedigitalcollection.asme.org/appliedmechanicsreviews/article-abstract/56/1/1/463637?casa_token=TKoefEXSKcMAAAAA:W_vey-ZmGi4NjDX5m2C6gh_57Bgipc5uaiqbiNatmMO6_NcD1CnPczYjbNxxrcoYuqFojwrf.

[11] A. Turon et al. "Accurate simulation of delamination growth under mixed-mode loading using cohesive elements: Definition of interlaminar strengths and elastic stiffness". In: *Composite Structures* 92.8 (July 2010), pp. 1857–1864. ISSN: 02638223. DOI: 10.1016/j.compstruct.2010.01.012.

[12] Brian Lau Verndal. *Progressive Damage Simulation of Laminates in Wind Turbine Blades under Quasistatic and Cyclic Loading*. Tech. rep. 2015.

[13] B. F. Sørensen. "Delamination fractures in composite materials". In: *Modeling Damage, Fatigue and Failure of Composite Materials*. Elsevier Inc., 2016, pp. 213–240. ISBN: 9781782422860. DOI: 10.1016/B978-1-78242-286-0.00011-X.

[14] Brian L.V. Bak et al. "A simulation method for high-cycle fatigue-driven delamination using a cohesive zone model". In: *International Journal for Numerical Methods in Engineering* 106.3 (Apr. 2016), pp. 163–191. ISSN: 1097-0207. DOI: 10.1002/NME.5117. URL: https://onlinelibrary.wiley.com/doi/full/10.1002/nme.5117%20https://onlinelibrary.wiley.com/doi/abs/10.1002/nme.5117%20https://onlinelibrary.wiley.com/doi/10.1002/nme.5117.

[15] E. Farmand-Ashtiani, J. Cugnoni, and J. Botsis. "Specimen thickness dependence of large scale fiber bridging in mode I interlaminar fracture of carbon epoxy composite". In: *International Journal of Solids and Structures* 55 (Mar. 2015), pp. 58–65. ISSN: 0020-7683. DOI: 10.1016/J.IJSOLSTR.2014.03.031.

[16] S. M. Jensen et al. "Formulation of a mixed-mode multilinear cohesive zone law in an interface finite element for modelling delamination with R-curve effects". In: *Composite Structures* 216 (May 2019), pp. 477–486. ISSN: 02638223. DOI: 10.1016/j.compstruct.2019.02.029.

[17] *Standard Test Method for Mode I Interlaminar Fracture Toughness of Unidirectional Fiber-Reinforced Polymer Matrix Composites 1*. Tech. rep. URL: www.astm.org,.

[18] Paul W Harper and Stephen R Hallett. "Cohesive zone length in numerical simulations of composite delamination". In: (2008). DOI: 10.1016/j.engfracmech.2008.06.004.

[19] James R Reeder, Kevin Demarco, and Karen S Whitley. "The use of doubler reinforcement in delamination toughness testing". In: (). DOI: 10.1016/j.compositesa.2004.02.021. URL: www.elsevier.com/locate/compositesa.

[20] Guillem Gall Trabal et al. "Delamination toughening of composite laminates using weakening or toughening interlaminar patches to initiate multiple delaminations: A numerical study". In: *Engineering Fracture Mechanics* 273 (Oct. 2022). ISSN: 00137944. DOI: 10.1016/J.ENGFRACMECH.2022.108730.

[21] Bent F Sørensen et al. "DCB-specimen loaded with uneven bending moments". In: *Int J Fract* 141 (2006), pp. 163–176. DOI: 10.1007/s10704-006-0071-x.

[22] Stergios Goutianos and Bent F. Sørensen. "Fracture resistance enhancement of layered structures by multiple cracks". In: *Engineering Fracture Mechanics* 151 (Jan. 2016), pp. 92–108. ISSN: 0013-7944. DOI: 10.1016/J.ENGFRACMECH.2015.10.036.

[23] HT Hahn, RY Kim - Journal of Composite Materials, and undefined 1976. "Fatigue behavior of composite laminate". In: *journals.sagepub.com* 10 (1976), p. 156. URL: https://journals.sagepub.com/doi/pdf/10.1177/002199837601000205.

[24] Joris Degrieck and Wim Van Paepegem. "Fatigue damage modeling of fibre-reinforced composite materials: Review". In: *Applied Mechanics Reviews* 54.4 (2001), pp. 279–300. ISSN: 00036900. DOI: 10.1115/1.1381395.

[25] Brian L.V. Bak et al. *Delamination under fatigue loads in composite laminates: A review on the observed phenomenology and computational methods*. Nov. 2014. DOI: 10.1115/1.4027647.

[26] Guillem Gall Trabal et al. "An adaptive floating node based formulation for the analysis of multiple delaminations under quasi-static loading". In: *Composites Part A: Applied Science and Manufacturing* 156 (May 2022). ISSN: 1359835X. DOI: 10.1016/j.compositesa.2022.106846.

[27] Guillem Gall Trabal et al. "An adaptive floating node based formulation for the analysis of multiple delaminations under high cycle fatigue loading". In: *Composites Part A: Applied Science and Manufacturing* 160 (Sept. 2022). ISSN: 1359835X. DOI: 10.1016/j.compositesa.2022.107036.

[28] G. Alfano and M. A. Crisfield. "Finite element interface models for the delamination analysis of laminated composites: mechanical and computational issues". In: *International Journal for Numerical Methods in Engineering* 50.7 (Mar. 2001), pp. 1701–1736. ISSN: 1097-0207. DOI: 10.1002/NME.93. URL: https://onlinelibrary.wiley.com/doi/full/10.1002/nme.93.

[29] Jonas Kyneb et al. *Title: Improved Damage Tolerance of Composites by Promoting Multiple Delaminations-Quasi-static Loading*. Tech. rep. URL: http://www.engineering.aau.dk/.

[30] *Technical Data INF-114 INF-212 Infusion epoxy*. Tech. rep. URL: https://www.prosetepoxy.com/wp-content/uploads/INF-114_INF-212.pdf.

[31] B L V Bak and E Lindgaard. *Automated digital image-based tracking of delamination fronts in translucent laminated materials*. Tech. rep.

[32] S. M. Jensen et al. "Transition-behaviours in fatigue-driven delamination of GFRP laminates following step changes in block amplitude loading". In: *International Journal of Fatigue* 144 (Mar. 2021). ISSN: 01421123. DOI: 10.1016/j.ijfatigue.2020.106045.

[33] B.F. Sørensen and T.K. Jacobsen. "Crack growth in composites Applicability of R-curves and bridging laws". eng. In: *Plastics, rubber & composites* 29.3 (2000), pp. 119–133. ISSN: 1465-8011. DOI: 10.1179/146580100101540879.

[34] Calvin Rans, René Alderliesten, and Rinze Benedictus. "Misinterpreting the results: How similitude can improve our understanding of fatigue delamination growth". In: (2010). DOI: 10.1016/j.compscitech.2010.11.010.